Theses and Dissertations   1. Thesis and Dissertation Collection, all items

1996-03

Studies in satellite multispectral determination of boundary layer depth

Teadt, Troy L.

Monterey, California. Naval Postgraduate School

http://hdl.handle.net/10945/9022

NAVAL POSTGRADUATE SCHOOL
MONTEREY, CALIFORNIA

THESIS

STUDIES IN SATELLITE MULTISPECTRAL
DETERMINATION OF BOUNDARY LAYER
DEPTH

by

Troy L. Teadt

March, 1996

Thesis Advisor: Carlyle H. Wash

Approved for public release; distribution is unlimited.

REPORT DOCUMENTATION PAGE

Form Approved OMB No. 0704-0188

1. AGENCY USE ONLY *(Leave blank)*	2. REPORT DATE March 1996	3. REPORT TYPE AND DATES COVERED Master's Thesis	
4. TITLE AND SUBTITLE STUDIES IN SATELLITE MULTISPECTRAL DETERMINATION OF BOUNDARY LAYER DEPTH		5. FUNDING NUMBERS	
6. AUTHOR(S) Troy L. Teadt			
7. PERFORMING ORGANIZATION NAME(S) AND ADDRESS(ES) Naval Postgraduate School Monterey CA 93943-5000		8. PERFORMING ORGANIZATION REPORT NUMBER	
9. SPONSORING/MONITORING AGENCY NAME(S) AND ADDRESS(ES)		10. SPONSORING/MONITORING AGENCY REPORT NUMBER	

11. SUPPLEMENTARY NOTES The views expressed in this thesis are those of the author and do not reflect the official policy or position of the Department of Defense or the U.S. Government.

12a. DISTRIBUTION/AVAILABILITY STATEMENT Approved for public release; distribution is unlimited.	12b. DISTRIBUTION CODE

13. ABSTRACT *(maximum 200 words)*

Satellite derived images of boundary layer properties are generated from AVHRR data collected during SHAREM 110 (6 February-18 February 1995) and during Naval Postgraduate School cruise (16 May 1995) for comparison with in-situ data. The technique, proposed by Kren (1987), verified by Smolinski (1988) and applied by Walsh (1994) uses NOAA AVHRR channels 1, 2, 4 and 5 and the relationships between radiative extinction and relative humidity and atmospheric absorption and column water vapor. The percent of total atmospheric water vapor contained in the MABL is determined, via the method of Walsh (1994), and is provided to the algorithm. The technique successfully mapped boundary layer heights for two different coastal regimes, Persian Gulf and Monterey Bay region. The method failed in the Gulf of Oman region for a case strongly affected by continental influences containing a large concentration of land aerosols. The results also show that the algorithm is closely tied to the sea surface temperature and can only retrieve the layer depth most closely associated with the surface. Therefore, this technique cannot indicate the presence of elevated layers not associated with the surface.

14. SUBJECT TERMS Remote Sensing, AVHRR, Marine Atmospheric Boundary Layer, Multispectral			15. NUMBER OF PAGES 81
			16. PRICE CODE
17. SECURITY CLASSIFICATION OF REPORT Unclassified	18. SECURITY CLASSIFICATION OF THIS PAGE Unclassified	19. SECURITY CLASSIFICATION OF ABSTRACT Unclassified	20. LIMITATION OF ABSTRACT UL

NSN 7540-01-280-5500

Standard Form 298 (Rev. 2-89)
Prescribed by ANSI Std. 239-18 298-102

ii

STUDIES IN SATELLITE MULTISPECTRAL DETERMINATION OF BOUNDARY LAYER DEPTH

Troy L. Teadt
Lieutenant, United States Navy
B.S., University of Arizona, 1984

Submitted in partial fulfillment
of the requirements for the degree of

MASTER OF SCIENCE IN METEOROLOGY AND PHYSICAL OCEANOGRAPHY

from the

NAVAL POSTGRADUATE SCHOOL
March 1996

ABSTRACT

Satellite derived images of boundary layer properties are generated from AVHRR data collected during SHAREM 110 (6 February - 18 February 1995) and during a Naval Postgraduate School cruise (16 May 1995) for comparison with in-situ data. The technique, proposed by Kren (1987), verified by Smolinski (1988) and applied by Walsh (1994) uses NOAA AVHRR channels 1, 2, 4 and 5 and the relationships between radiative extinction and relative humidity and atmospheric absorption and column water vapor. The percent of total atmospheric water vapor contained in the MABL is determined, via the method of Walsh (1994), and is provided to the algorithm. The technique successfully mapped boundary layer heights for two different coastal regimes, Persian Gulf and Monterey Bay region. The method failed in the Gulf of Oman region for a case strongly affected by continental influences containing a large concentration of land aerosols. The results also show that the algorithm is closely tied to the sea surface temperature and can only retrieve the layer depth most closely associated with the surface. Therefore, this technique cannot indicate the presence of elevated layers not associated with the surface.

TABLE OF CONTENTS

ACKNOWLEDGMENTS

I wish to express my gratitude to several people whose help and support were instrumental in the completion of this thesis. Professors Carlyle Wash and Kenneth Davidson for their guidance and encouragement necessary to turn an idea into a thesis. Mary Jordan for her computer assistance. Kurt Nielsen for the instruction on the finer points of TERASCAN. Without their help this thesis would not have been a success. Most importantly, I wish to thank my wife, Heidi, for her support and understanding during this project.

I. INTRODUCTION

U. S. Navy operational philosophy has changed
dramatically in the past five years. Operations have gone
from blue water to littoral and from battlegroup to small
groups and independent units. This change in operating
procedures has greatly increased the challenges facing
Commander, Meteorology and Oceanography Command in providing
environmental support, especially in the arena of
electromagnetic (EM) propagation forecasting. The use of
basin-wide estimates or homogeneous atmosphere models will
not be acceptable in future operations and conflicts.

The single radiosonde is not enough to predict the
downrange atmosphere which controls how the EM energy will
propagate. The atmospheric parameters which affect ducting
and EM propagation vary so greatly, spatially and
temporally, that it would be physically prohibitive
to characterize them with current instrumentation,
radiosondes.

An effort has begun to quantify and predict ducting
phenomena by satellite methods. The IR Duct technique
(Rosenthal and Helvey 1992) allows one to estimate the
height of the top of a trapping layer for stratus regions.

Multispectral techniques (Kren 1987, Smolinski 1988 and Walsh 1994), can yeild estimates of the marine atmospheric boundary layer (MABL) depth for clear regions.

The map of MABL depth estimates, provided by the multispectral technique, is a key tool in the intelligent estimating of EM propagation for the area of interest. This is very promising for operations in areas where the atmospheric parameters responsible for determining the MABL height display large spatial variability, as in the littoral, and for independent operations when large battlegroup assets are not available.

To date the study of the multispectral technique has been largely developed with data from the eastern North Pacific Ocean off the coast of Southern California, the California Bight. This investigation will encompass two quite different climotological regions: the Persian Gulf, using data from SHAREM 110, and the Eastern North Pacific Ocean, using data of opportunity. The purpose of this thesis will be:

- to construct satellite derived images of boundary layer height using the Kren/Smolinski/Walsh algorithm.

- to evaluate the usefulness of the above images with comparisons with the in-situ radiosondes.

- to evaluate the ability to use this technique in climotological regions outside of the California Bight.

II. BACKGROUND

A. REMOTE SENSING OF BOUNDARY LAYER DEPTH

Kren (1987) presented a method for estimating the MABL depth and surface relative humidity by exploiting the relationships between relative humidity and radiative extinction and atmospheric absorption and column water vapor. This method uses measurements of aerosol optical depth, total water vapor and SST from the same satellite sensor. This eliminates resolution conflicts and the need for data integration. This method contains three necessary assumptions in order to be accurate: 1) the MABL must be well-mixed, 2) all aerosols contributing to radiative extinction must be located in the MABL, 3) the percentage of water vapor contained in the MABL can be estimated.

Smolinski (1988) confirmed the approach of Kren (1987), as well as, incorporating a technique to spatially map the boundary layer height. Smolinski (1988) noted in his study that the technique for estimating humidity showed a positive bias in overestimating the MABL depth due to a portion of the total water vapor being above the MABL.

Walsh (1994) was able to relax the assumption that the total atmospheric water vapor is confined to the MABL. He

integrated absolute humidity to 10 km and then found the percent confined to a predetermined MABL height, as determined from a local sounding. This calculated percentage was then incorporated into the MABL height calculation. He was then able to successfully map the MABL over a coastal region, using multispectral AVHRR data obtained during the Variability Of Coastal Atmospheric Refractivity Intensive Observation Period (VOCAR IOP) using the Kren/Smolinski iterative technique. The reader is referred to Walsh (1994) for more details on this technique.

Studies in the use of satellite multispectral MABL height retrievals have continued since 1994. These studies have focused on the subsidence region of the subtropical gyre over the California Bight. This paper intends to examine the applicability of this technique for other locations around the world. The areas examined are the Persian Gulf/Gulf of Oman, with data being obtained from SHAREM 110, and the Eastern North Pacific Ocean from a cruise data collection period conducted by the Naval Postgraduate School (NPS).

The multispectral methods are not applicable to cases when stratus occurs in the MABL. Rosenthal and Helvey (1992) developed the IR Duct technique, an empirical method to determine boundary layer depth for a region covered with

stratus cloud formations. By subtracting the IR derived cloud-top temperature, retrieved from AVHRR channel 4, from the in-situ SST and dividing by a lapse rate of 8.5 °C per kilometer they found that general estimates of the MABL height could be made.

B. SHAREM 110

The Ship Antisubmarine Warfare Readiness/Effectiveness Measuring (SHAREM) program was established by Chief of Naval Operations in 1969 with the specific objectives of:
1) constructing exercises to support Fleet Commander's Goals, 2) gathering high quality data, 3) identifying tactical problems and produce tactical guidance/recommendations, 4) developing and maintaining historical SHAREM database. Through the 1970's and 80's the emphasis of the SHAREM has been on sonar and acoustic developments but more recently the development of Electromagnetic/Electro-Optical (EM/EO) systems have become increasingly important. SHAREM 110 was designed to test/demonstrate capabilities of EM/EO support system currently under development and to identify system performance problems impacted by the physical environment.

SHAREM 110 occurred in the Arabian Gulf and the Gulf of Oman from 6 to 18 February 1995. 119 radiosondes, 28

rocketsondes and 15 dropsondes were launched by the three
surface ships involved in the exercise. To complete the
atmospheric database 390 hourly automatic meteorological and
oceanographic (METOC) observations were taken, 6
meteorological research flights by a United Kingdom C-130
were made and 288 hours of aerosol measurements were
recorded.

A total of five satellite passes (NOAA 14) were
collected during the exercise at NPMOD Bahrain. All five
AVHRR channels were archived:

- Channel 1, 0.58 - 0.68 μm, red-visible,
- Channel 2, 0.72 - 1.10 μm, red-visible/near infrared,
- Channel 3, 3.55 - 3.93 μm, near infrared
- Channel 4, 10.3 - 11.3 μm, thermal infrared
- Channel 5, 11.5 - 12.5 μm, thermal infrared.

The AVHRR data was radiometrically calibrated, yielding
percent albedo units for channels 1 and 2 and brightness
temperature for channels 3 to 5.

The satellite passes that were collected were then
screened for two basic criteria: 1) did the pass cover the
in-situ measurement area? 2) was the area in question clear
and not cloud covered?

The first pass occurred at 0912Z 7 February 1995 but
due to a cold front moving through, the area was covered

8

with cumulus clouds. The second pass was at 1021z 10 Feb. and yielded a clear image of the area in question. The third pass only covered the Gulf of Oman and not the area of the in-situ measurement. The fourth pass, at 0937Z 14 Feb., produced a clear image of the in-situ measurement area. The fifth and last pass was collected at 0854z 18 Feb. and yielded a cloud covered image of the area of interest.

C. NPS DATA COLLECTION OPPORTUNITIES

The Naval Postgraduate School (NPS), located in Monterey, California, has the resources to locally receive and archive satellite data. NPS also has access to the RV Pt Sur, a National Science Foundation research vessel, for coastal measurement cruises. This combination gives NPS many unique opportunities to collect atmospheric data across the Eastern North Pacific.

This presented some opportunities to evaluate the multispectral satellite technique for satellite passes that met the algorithm's criteria. One such opportunity occurred on 16 May 1995. The RV Pt Sur was located near the mouth of Monterey Bay and another ship, the RV McArthur, a NOAA ship, was located several miles northwest of the RV Pt Sur. Both ships made several radiosonde launches throughout the day.

9

Two soundings from each ship corresponded with satellite passes from NOAA 12, at 1512z, and NOAA 14, at 2204z. Both images indicate clear conditions over Monterey Bay.

III. RESULTS OF SATELLITE ANALYSIS

A. APPROACH

The satellite data are checked for clear skies over the in-situ collection point and if this is true the case is selected for examination. The in-situ radiosonde data that are closest in time to the satellite pass are first compared and then soundings that are further removed temporally are then included. If the pass is partially obscured by cloud and there are in-situ data available in the cloudy area an alternate method, IR duct, may be used in the comparison.

Based on the selection criteria, two specific satellite passes from SHAREM 110 and two passes from a NPS cruise were selected for intensive examination. The passes during SHAREM 110 occurred on 10 February 1995 and 14 February 1995. The passes during the NPS cruise occurred on 16 May 1995. A detailed comparison of satellite-derived and in-situ observed data are given in the following sections.

B. SHAREM 110 CASE 1: 10 FEBRUARY 1995

1. MABL Characteristics

Sounding data from the USS David R. Ray and the USNS Silas Bent were used to determine the thermal and moisture characteristics in and above the MABL from 0600Z through

11

1200Z on 10 February. During this time period the ships were in the Persian Gulf. Due to the geography of the Persian Gulf, the atmosphere is never completely free from land influences. However, during this time the mean atmospheric flow was from the northwest gave a minimal continental influence over the area. Figures 1(a), 2(a), and 3(a) show three vertical soundings of temperature and dew point temperature versus height at 06z, 09z and 12z on 10 February from the USNS Silas Bent and the USS David R. Ray. Figures 1(b), 2(b) and 3(b) show three vertical water vapor profiles from the corresponding soundings. An examination of the figures shows:

- The boundary layer is well mixed during this period, as is required by the initial assumptions of the algorithm; note the nearly vertical dew point temperature profiles and the nearly vertical water vapor profiles,

- The top of the boundary layer is well defined by an increase in temperature, a large drop in dew point temperature and a corresponding sharp drop in water vapor pressure,

- Although 100 percent of the water vapor is not located in the boundary layer a significant majority is, approximately 83 percent,

- The boundary layer is quite deep, on the order of 1000 meters, with the atmosphere drying rapidly above it,

- The temperature and moisture variables are in excellent agreement as to the boundary layer height,

12

2. Visible and Infrared Satellite Images

An examination of the AVHRR Channel 1 visible for the 1021z pass on February 10th, Figure 4, shows a fairly clear region with a cumulus-stratocumulus band across the southwest corner. The 06z and 09z soundings provided by the USNS Silas Bent and the USS David R. Ray are in the clear. The 12z sounding provided by the USS David R. Ray is in the stratocumulus.

The AVHRR Channel 4 infrared image, Figure 5, indicates the warmest regions along the coast as is expected in a daytime pass; these areas are imaged black. The cumulus cloud band across the southwest of the image is the coldest, followed by the neighboring stratocumulus; which is significantly cooler than the warm Persian Gulf Water.

3. Sea Surface Temperature Image

Figure 6 displays the satellite-derived sea surface temperatures (SST), which indicates a fairly uniform sea surface temperature across the region. The cooler temperatures indicated near the clouds are suspect due to probable cloud contamination of the samples. Temperatures across the area of interest lie in the 20 to 22 °C range.

Satellite-derived SST's using the NOAA/NESDIS operational algorithm were compared with the in-situ measurements from the USNS Silas Bent. The accuracy of this

estimate is important as a bottom boundary condition for the iterative scheme. The difference was 0.88 °C. Table I contains the derived and in-situ SST comparison. It is noted that the only in-situ SST data available was from the USNS Silas Bent, The USS David R. Ray did not record the SST data for this time period.

4. Optical Depth

Figure 7 displays the satellite derived optical depth of the SHAREM 110 region at 1021z, 10 February 1995. The image displays a fairly uniform optical depth over the area not affected by clouds. The retrieved optical depths for the USNS Silas Bent and the USS David R. Ray are 0.20 and 0.21 respectively.

5. Boundary Layer Height Image

The boundary layer height image, Figure 8, displays a fairly constant MABL height across the area. This is consistent with the uniform optical depths. Since the height of the boundary layer is a function of optical depth, as pointed out by Walsh (1994), then any variation in optical depth would be reflected in the boundary layer height image. The satellite analysis indicates that MABL heights generally range between 0.9 km and 1.25 km across this area of the Persian Gulf.

14

The relative accuracy of the satellite derived data was evaluated. The study conducted by Smolinski (1988) utilizing several different (simulated) boundary layers yielded standard deviations of boundary layer height ranging from 95 to 169 m. The study by Walsh (1994), where satellite derived boundary layer height was brought into agreement with offshore radiosonde measurements by varying the total amount of water vapor in the MABL, yielded average boundary layer height errors of 31 m, ranging from 5 to 210 m, for one case and 57 m, ranging from 41 to 113 m, for the other. In this case, the satellite-derived boundary layer height was directly compared to the shipboard radiosonde measurements. The average error for this comparison was 49 m.

Unlike the procedures performed by Walsh (1994) the satellite-derived boundary layer height was not made to agree with the shipboard radiosonde measurements by adjusting the amount of total water vapor confined to the MABL. The total amount of water vapor confined to the MABL was computed to be 83 percent as determined from the USS David R. Ray 09z sounding. The satellite algorithm was run using this water vapor figure and then compared to the radiosonde determined height for 09z and 06z. Table II shows the results of the boundary layer height comparisons.

15

At 12z the USS David R. Ray had moved under the stratocumulus deck as indicated in Figure 5. Since this violates the primary assumption of the algorithm, cloud free conditions, the 12z sounding was not deemed useful in comparing with the satellite-derived boundary layer heights. However, the IR duct technique was employed to examine the ability to use the same satellite data for both techniques concurrently. The difference between the radiosonde derived boundary layer height and that determined by the this technique was 33 m. Table III contains the results of this comparison. The fact that MABL depth from the cloud top temperatures are consistent with multispectral estimates provides additional confirmation of the MABL analysis.

C. SHAREM 110 CASE 2: 14 FEBRUARY 1995

1. MABL Characteristics

Sounding data from the USS Lake Erie and the USNS Silas Bent were used to determine the thermal and moisture characteristics in and above the MABL at 09z on 14 February. During this time period the ships were in the Gulf of Oman. Again, due to the land surrounding this water mass, offshore influences are very common. During this time the atmospheric flow in the boundary layer was from the northeast coming directly off Iran, with a typically very

16

warm and dry resident air mass. Figures 9(a), and 10(a) show two vertical soundings of temperature and dew point temperature versus height at 09z on 14 February. Figures 9(b), and 10(b) show two vertical water vapor profiles from the corresponding soundings. An examination of the figures shows:

- The boundary layer is well mixed at the time it was sampled, as is required by the initial assumptions of the algorithm; note the nearly vertical dew point temperature profiles and the nearly vertical water vapor profiles,

- The top of the boundary layer is well defined by an increase in temperature, a large drop in dew point temperature and a corresponding sharp drop in water vapor pressure,

- The atmosphere is very dry, as indicated by the near surface dew point temperatures of less than 0 °C and a maximum vapor pressure of less than 6 hPa,

- Although the atmosphere is very dry there is a significant portion of the total water vapor contained above the MABL, with a slight majority in the MABL, approximately 55 percent,

- The boundary layer is very deep, nearly 1000 meters,

- The variables are in excellent agreement as to the boundary layer height,

2. Visible and Infrared Satellite Images

Figure 11 is an enhanced AVHRR Channel 1 visible image taken from a 0937z pass on February 14th. What stands out in this image are the two plumes extending from the coast of

17

Iran towards the southwest, one extending over the USNS Silas Bent and another to the east-northeast of the USS Lake Erie. The plumes seem to be emanating from two river valleys, the Jagin and Rapch, which split the rugged terrain of southern Iran. The meteorological observations reported by the ships at 09z indicate winds from the northeast at 15 to 20 knots, which is consistent with winds being funneled out of these valleys. This strongly supports the fact that these plumes are dust or sand being advected off Iran. This is also consistent with the very warm and dry atmospheric profiles.

Figure 12 presents an enhanced AVHRR Channel 4 infrared image for this period. Again the warmest regions are over land. The two plumes are evident in the IR temperature image also. However, examining the enhancement indicates the brightness temperature difference between the USNS Silas Bent, within the plume, and the USS Lake Erie, outside the plume, is only 0.3 °C. This indicates a small amount of absorption at some small altitude above the surface, another indication that the plumes are most likely dust.

3. **Sea Surface Temperature Image**

The SST image, Figure 13, displays a rather uniform SST pattern across the Gulf. The temperatures are higher than observed within the Persian Gulf, ranging from 22 to 24 °C,

18

1.5 to 2 °C higher. However, there are distinct indications
of cooler water being upwelled along the southern coast of
Iran. This would be consistent with the strong off shore
flow pushing the warmer surface water away from the land and
towards the center of the Gulf of Oman.

Satellite-derived SST's using the NOAA/NESDIS
operational algorithm were compared with those from the USNS
Silas Bent and the USS Lake Erie. The average error was
0.36 °C, with the error measured at the USNS Silas Bent (in
the dust plume) being 0.69 °C and that measured at the USS
Lake Erie only 0.03 °C, as shown in Table I.

4. Optical Depth

Figure 14 displays optical depth as derived from the
satellite data. There are two areas of increased optical
depth, corresponding to the plumes described previously.
The optical depth within the plumes is greatest near the
shore and decreases away from the land, very consistent with
a land based aerosol being advected seaward. Also, a marine
environment would tend to produce very uniform optical
depths, as seen in Figure 7, vice the variability displayed
in this image. The area around the USNS Silas Bent, which
is within one of the plumes, has an optical depth of 0.22,
whereas, the area around the USS Lake Erie, outside of the
plumes, has an optical depth of 0.18.

During SHAREM 110 the USS Lake Erie made in-situ measurements of cloud condensation nuclei (CCN). Goroch and Raby (1995) report that while in the Gulf of Oman the measured CCN concentrations were consistently in excess of 10,000 particles per cubic centimeter. Normal, open ocean, CCN concentrations are measured in the thousands of particles per cubic centimeter. Clearly the aerosol concentrations across the Gulf of Oman were aloft and this has led to the increased optical depths. Although the USS Lake Erie did not measure CCN concentrations within the plumes it can be expected that the CCN concentrations would be even higher in those areas.

5. Boundary Layer Height

The satellite-derived boundary layer height (not shown) was directly compared to the shipboard radiosonde measurements. The average error for this comparison was 353 m, with an error of 492 m as measured from the USNS Silas Bent and 213 m as measured from the USS Lake Erie. The satellite-derived heights were lower than the radiosonde computed heights as shown in Table II.

It is quite surprising the technique actually converged in this case. The data clearly indicates that the environment is dominated by continental influences vice marine. Since the basis of the technique is the

20

relationship between extinction and relative humidity (Durkee, 1984) for a marine layer and not a continental one, the technique is not expected to be successful. This case illustrates the need to carefully monitor the environment in an offshore flow situation. If continental influences dominate the environment this technique cannot be applied.

D. CENTRAL CALIFORNIA COAST, CASE 1: 1500z, 16 MAY 1995

1. MABL Characteristics

The second area investigated in this thesis is the Central California Coast near Monterey Bay. Sounding data from the RV Pt Sur was used to determine the thermal and moisture characteristics in and above the MABL at 15z on 16 May. During this time period the ship was in the mouth of Monterey Bay. During this time the mean atmospheric flow was from the northwest which plays a key role in initiating upwelling events along the coast. Figure 15(a) and (b), show a vertical sounding of temperature and dew point temperature versus height and the vertical water vapor profile at 15z on 16 May. Figure 16, is the profile of mixing ratio versus height from the corresponding sounding.

An examination of the figures shows:

- There is some ambiguity as to the top of the boundary layer. There are two layers, one at 139 m and 450 m, defined by a drop in dew point

21

temperature and a corresponding drop in water vapor
pressure,

- Examining the mixing ratio profile assists in
  determining the true MABL as the lowest layer,

- It is uncertain if the boundary layer is well
  mixed at the time it was sampled,

- The atmosphere is very moist above the MABL with
  only 7.34 percent of the total water vapor
  residing in the boundary layer, as indicated by
  the vapor pressure profile,

- The boundary layer is very shallow, approximately
  150 meters,

2. Visible and Infrared Satellite Images

Figure 17 presents a NOAA 12 AVHRR Channel 1 visible
image taken from a 1512z pass on May 16th. There are
several bands of cumulus and stratocumulus clouds covering
the northwestern portion of the image, however, the Monterey
Bay area is clear.

Figure 18 is a NOAA 12 AVHRR Channel 4 infrared image.
The warmest regions are over land and are therefore the
darkest on the image. The strong convective bands to the
west and northwest of Monterey Bay are quite evident from
their very bright, cold, tops. Again, Monterey Bay is
clear. There is some evidence of cooler temperatures along
the coast, a possible indication of cooler sea surface
temperatures caused by an upwelling event.

Convective activity over Monterey Bay may very well be suppressed by some slight subsidence at approximately 2000 m as indicated in Figure 15. A weakening of the subsidence seaward would allow the convection to the west and northwest of Monterey Bay to occur.

3. Sea Surface Temperature Image

The SST image, Figure 19, displays some definite variability in the Monterey Bay area. There are cooler SST values along the coast with warmer values farther offshore. This is a fairly common occurrence in this region when a northwesterly atmospheric flow produces an offshore Ekman transport in the ocean and causes upwelling along the coast as the surface waters are pushed seaward. Temperatures in this area range from 11 to 14 °C.

Satellite-derived SST's using the NOAA/NESDIS operational algorithm were compared with those from the RV Pt Sur. The average difference was 0.58 °C. Table IV contains the result of the SST comparison.

4. Boundary Layer Height Image

The boundary layer height image, Figure 20, displays a fairly uniform MABL height across the Monterey Bay region. MABL heights generally range between 0.12 km and 0.20 km across the area.

The satellite-derived boundary layer height was directly compared to the shipboard radiosonde determined height. The average error for this comparison was 7 m. The error is due to the satellite-derived height being lower than the radiosonde determined height, as shown in Table V.

Figure 21 displays the M profile of the RV Pt Sur 1500z sounding. There are clearly multiple layers indicated in this refractive profile. Since the algorithm uses the SST as its bottom boundary condition it can only retrieve the layer immediately above the surface. Therefore, the technique will not yield any information about elevated layers not sdjacent to the satellite-measured SST.

E. CENTRAL CALIFORNIA COAST, CASE 2: 2200z, 16 MAY 1995

1. MABL Characteristics

Sounding data from the NOAA ship, RV McArthur, was used in conjunction with data from the RV Pt Sur to determine the thermal and moisture structure in and above the MABL later in the day, 22z, on 16 May. During this time period the RV Pt Sur has moved approximately 9 miles to the southwest from its 15z position. The RV McArthur was approximately 40 miles to the northwest of the RV Pt Sur. During this time the mean atmospheric flow was still from the northwest.

24

Figure 22(a) and (b) show the vertical soundings of temperature and dew point temperature versus height and the vertical water vapor profiles at 22z on 16 May reported at the RV Pt Sur. It is quite evident that the surface data reported by the radiosonde is in error, producing elevated dew point and water vapor values. Figure 23(a) and (b) show the vertical soundings of temperature and dew point temperature versus height and the vertical water vapor profiles at 22z on 16 May reported at the RV McArthur. Figure 24 and 25, are the profiles of mixing ratio versus height from the corresponding soundings. An examination of the figures shows:

- The top of the boundary layer is very ambiguous in the McArthur sounding, however, it is more clear in the Pt Sur sounding at 228 m. The RV McArthur sounding may be more well mixed due to its proximity to convective activity prominent on satellite imagery,

- Examining the mixing ratio profiles assists in determining the true MABL as the lowest layer,

- The boundary layer at the RV Pt Sur is more well mixed and deeper now than earlier in the day,

- The atmosphere is very moist above the MABL with only 13.63 percent of the total water vapor residing in the boundary layer, as indicated by the vapor pressure profile,

2. Visible and Infrared Satellite Images

Figure 26 is a NOAA 14 AVHRR Channel 1 visible image taken from a 2204z pass on May 16th. There are several patches of cumulus and stratocumulus clouds over the northern and northwestern portion of the image, near the RV McArthur's position, but it is clear over Monterey Bay and seaward for quite a distance.

Figure 27 is a NOAA 14 AVHRR Channel 4 infrared image. The warmest regions are over land and are therefore the darkest on the image. The strong convective areas to the north and northwest of Monterey Bay are quite evident from their very bright, cold, tops. There is, again, some evidence of cooler temperatures along the coast, in agreement with the morning imagery.

3. Sea Surface Temperature Image

The SST image, Figure 28, displays a continuing pattern of upwelling along the coast. The area of cooler water has expanded to include most of the coast and the majority of Monterey Bay. Temperatures in the area of the RV Pt Sur and RV McArthur range from 12 to 14 °C.

Satellite-derived SST's using the NOAA/NESDIS operational algorithm were compared with those from the RV Pt Sur and the RV McArthur. The average error was 0.24 °C,

with the error at the RV Pt Sur of 0.36 °C and the error at the RV McArthur of 0.12 °C, as shown in Table IV.

4. Boundary Layer Height Image

The boundary layer height image, Figure 29, displays a height pattern which slopes upward away from the coast. MABL heights generally range between 0.20 km and 0.30 km across this area.

The satellite-derived boundary layer height was directly compared to the shipboard radiosonde measurements. The average error for this comparison was 15.5 m, the error at the RV Pt Sur being 22 m and the error at the RV McArthur being 9 m. The error is due to the satellite-derived height being higher than the radiosonde computed height. Table V contains the results of these comparisons.

Figure 30(a) and (b) are the M profiles of the 2200z, 16 May 1995, soundings of the RV Pt Sur and the RV McArthur respectively. Again, note the multiple layers indicated. Each layer influences EM/EO propagation and may be tactically significant. This technique can yield information about only one layer, the layer closest to the surface.

28

IV. CONCLUSIONS

The marine atmospheric boundary layer (MABL) depth was successfully mapped out over areas outside of the California Bight using multispectral satellite data. The Persian Gulf, Gulf of Oman and the Monterey Bay coastal region were mapped utilizing data acquired during SHAREM 110 and a Naval Postgraduate School cruise. The iterative technique proposed by Kren (1987), validated by Smolinski (1988) and applied by Walsh (1994) was utilized. The original assumption that all water vapor must be confined to the MABL was relaxed through the methodology implemented by Walsh (1994) which determined the percent of total atmospheric water vapor confined to the MABL.

This study has shown the potential applicability of this technique to varied climotological regions and MABL depths. When applied to a very thick MABL over the Persian Gulf, approximately 1000 m, it produced an average error of 49 m, a 4.6 percent error. It was successfully applied to a very thin MABL over the Monterey Bay region, approximately 130 m increasing to approximately 220m, producing an average error of 12.6 m, a 5.8 percent error. Considering that operational radiosondes sample at approximately every 50 m

the differences produced in these cases are within the error
of the in-situ measurements.

However, some drawbacks to the technique were
discovered. The case study from the Gulf of Oman produced
satellite derived boundary layer heights several hundred
meters lower than the in-situ measurements. Due to the
strong advection of dry, dust laden, air from Iran the
optical depth over the target area was very high. The
algorithm is based on determining the boundary layer height
of a marine atmosphere. Therefore, the algorithm determined
that in order for a MABL to have the appropriate
concentrations of marine aerosols to produce such an optical
depth it must be much shallower than it truly was. This
result confirms that this technique cannot be applied when
the atmosphere is heavily affected by especially high
continental aerosol concentrations.

Another aspect of this technique portrayed in this
study is its inability to depict multiple layers in the
atmosphere. During the NPS cruise cases an upwelling event
is underway. The cold surface waters were modifying the
characteristics of the MABL and in essence forming a new
boundary layer. Since the multispectral algorithm is tied
to the satellite (IR) sensed SST, as its bottom boundary
condition, it will retrieve the layer depth most closely

associated with that SST, the lowest layer. For a simple MABL structure, as in the Persian Gulf case, this poses no problems. However, in a complex environment where new layers are evolving, care must be taken in determining where the actual MABL is located in the in-situ data. Since the percent of the total atmospheric water vapor contained in the MABL is input by the user, the incorrect identification of the MABL may lead to an erroneous solution or possible non-convergence of the algorithm. The environment may also be so complex as to not be classified as well-mixed. The key point is, regardless of the success or failure of the algorithm, this technique cannot determine elevated layers which are unassociated with the surface but may be tactically relevant to EM/EO propagation.

The IR technique, Rosenthal and Helvey (1992), was used in conjunction with the multispectral method during the first SHAREM 110 case. This, as pointed out by Walsh (1994), indicates continued potential for the integration of these two techniques to provide a more comprehensive coverage for areas where stratus clouds are frequently found.

Recommendations for further study are to: 1) conduct continued studies applying this technique to other areas of the world, 2) investigate the ability to remotely

determine the water vapor content above the boundary layer
thus leading to a complete satellite retrieval method, 3)
integrate the IR and multispectral techniques for a more
complete specification of the topography of the top of the
MABL.

APPENDIX

This appendix serves as a convenient location to consolodate all the figures discussed in the text of this thesis.
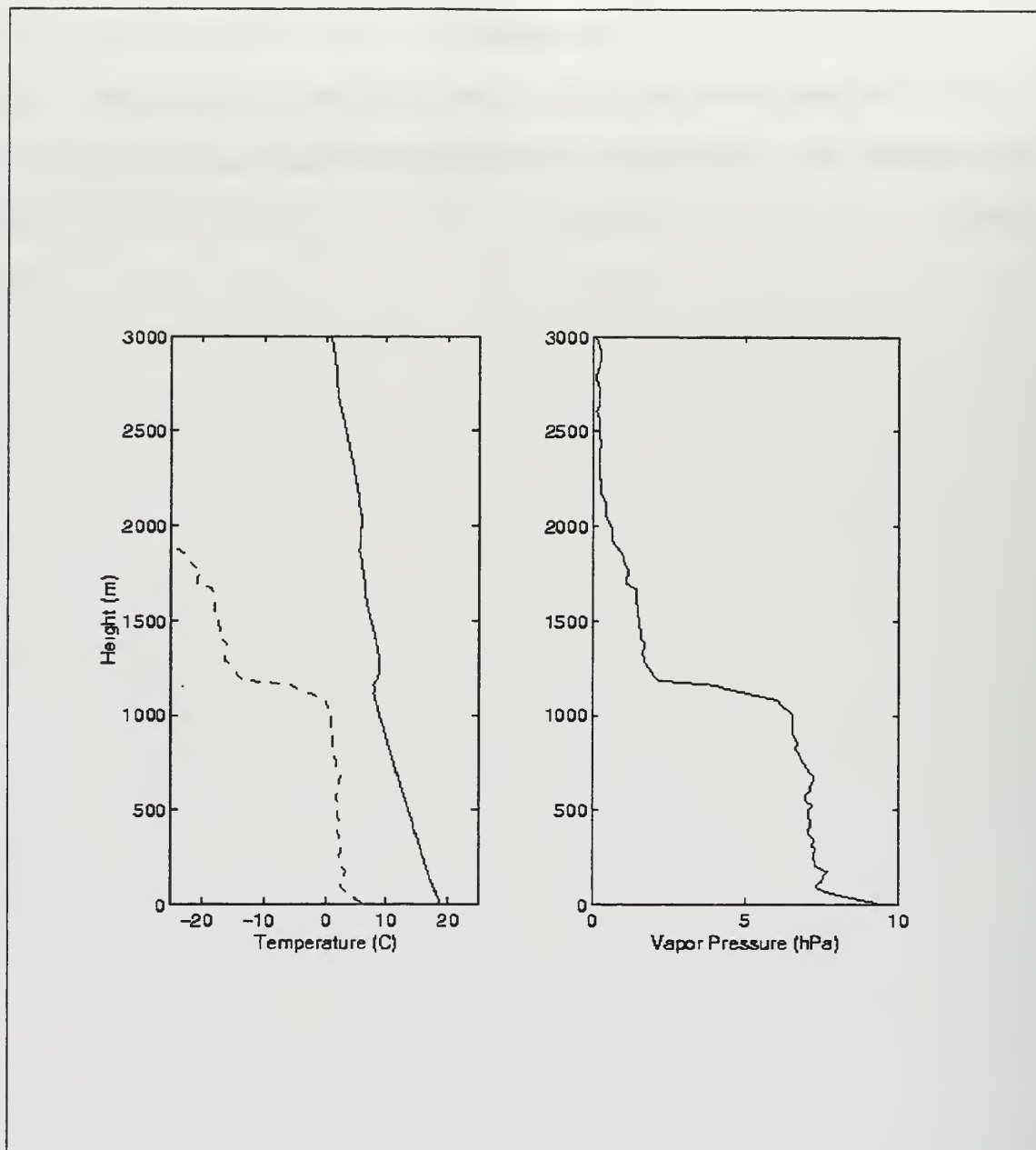
Figure 1: USNS Silas Bent, 0600z, 10 February. Fig. (a) shows vertical sounding and (b) shows vapor pressure versus height (m). Note the constant values of dew point and vapor pressure within the MABL. The boundary Layer is well-mixed.
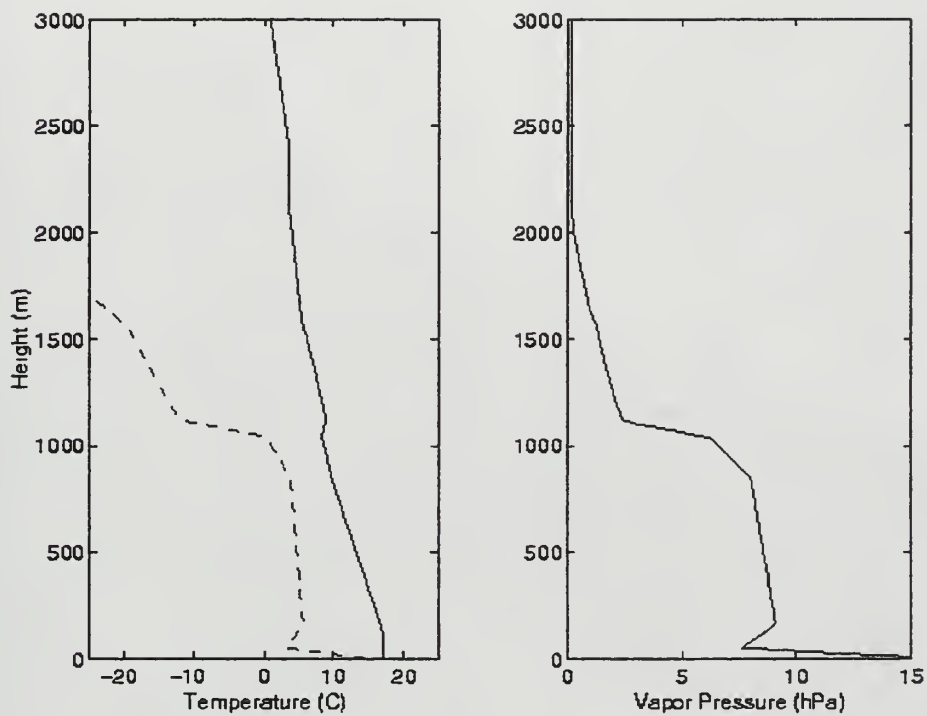
Figure 2: As in Figure 1 except for USS David R. Ray, 0900z, 10 February 1995.

35
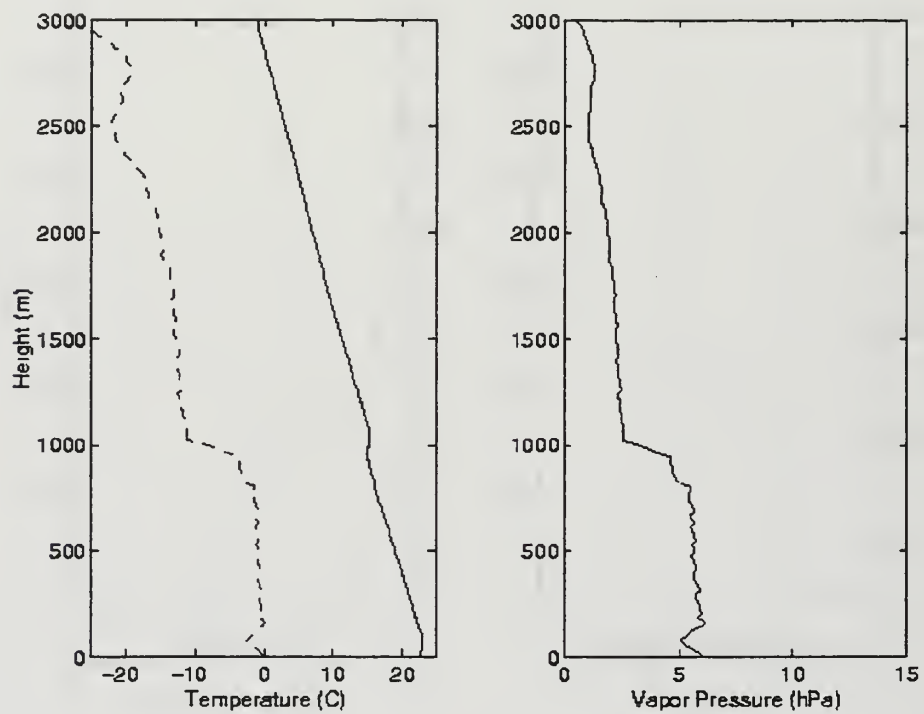
Figure 3: As in Figure 1 except for USS David R. Ray, 1200z, 10 February 1995.
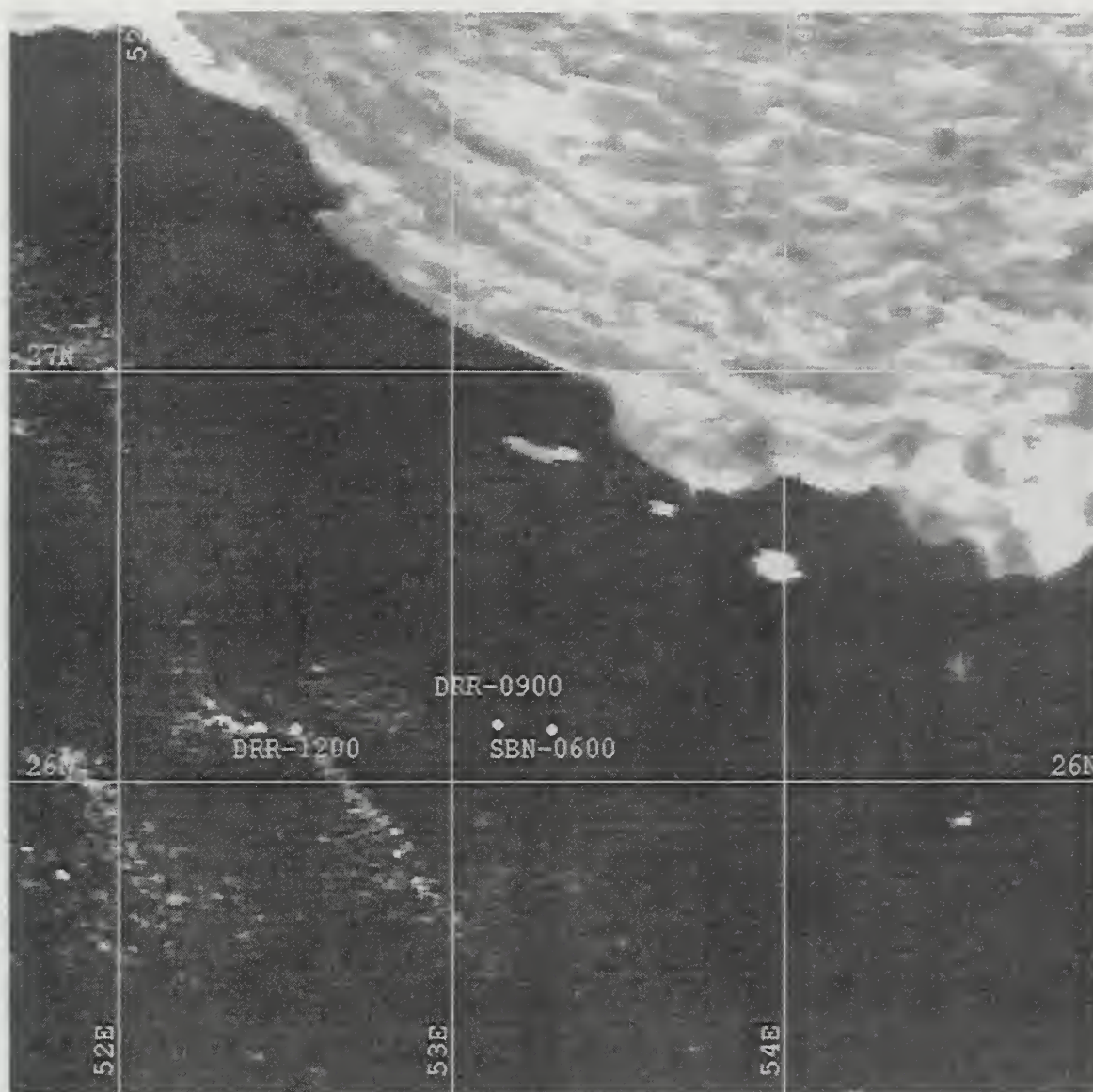
Figure 4: NOAA 14 AVHRR Channel 1 (visible) image of the
SHAREM 110 region at 1021z, 10 February 1995. Locations of
USNS Silas Bent (SBN) and USS David R. Ray (DRR) and the
time of soundings are indicated.
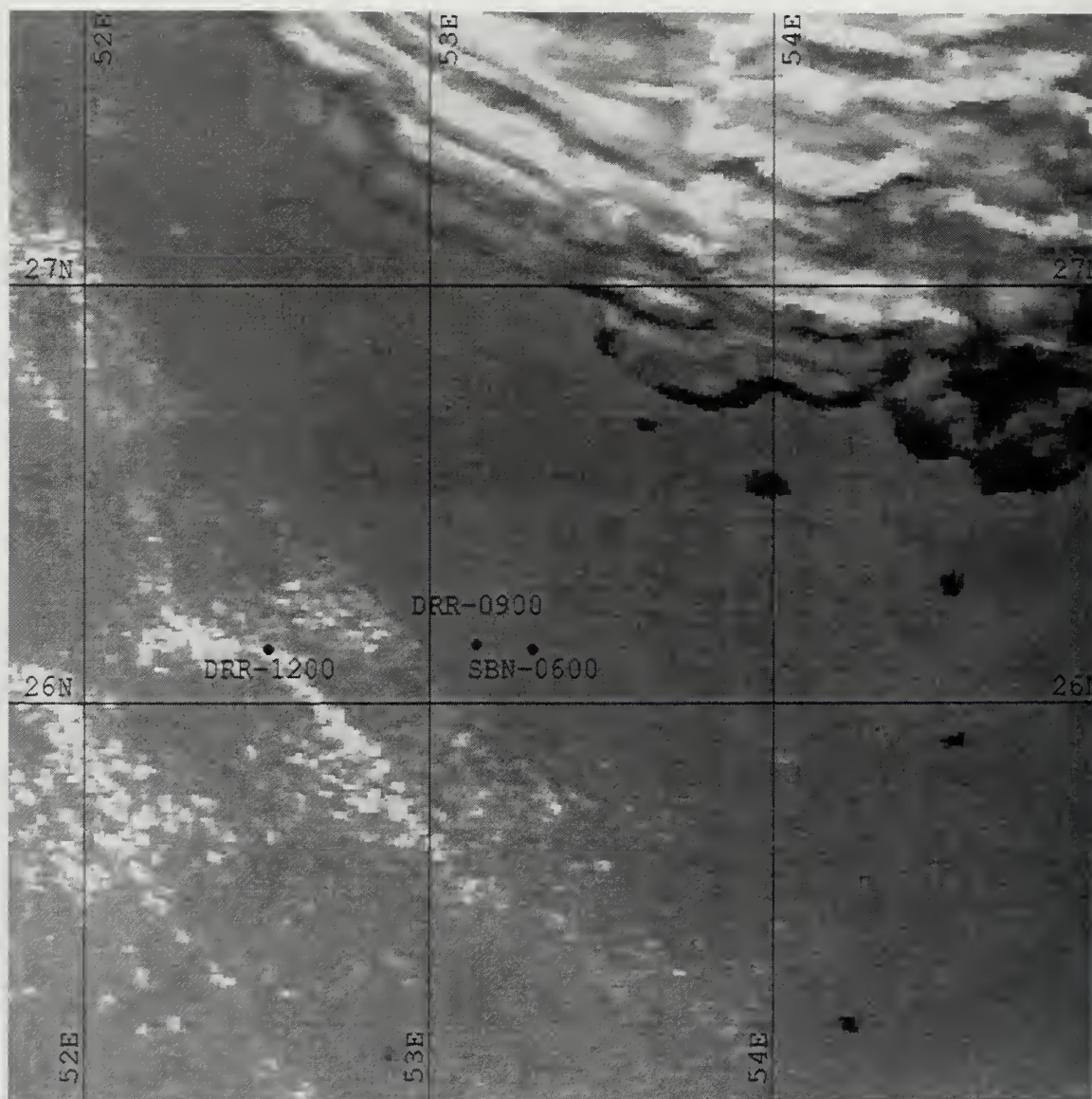
Figure 5: NOAA 14 AVHRR Channel 4 (infrared) image of the
SHAREM 110 region at 1021z, 10 February 1995.
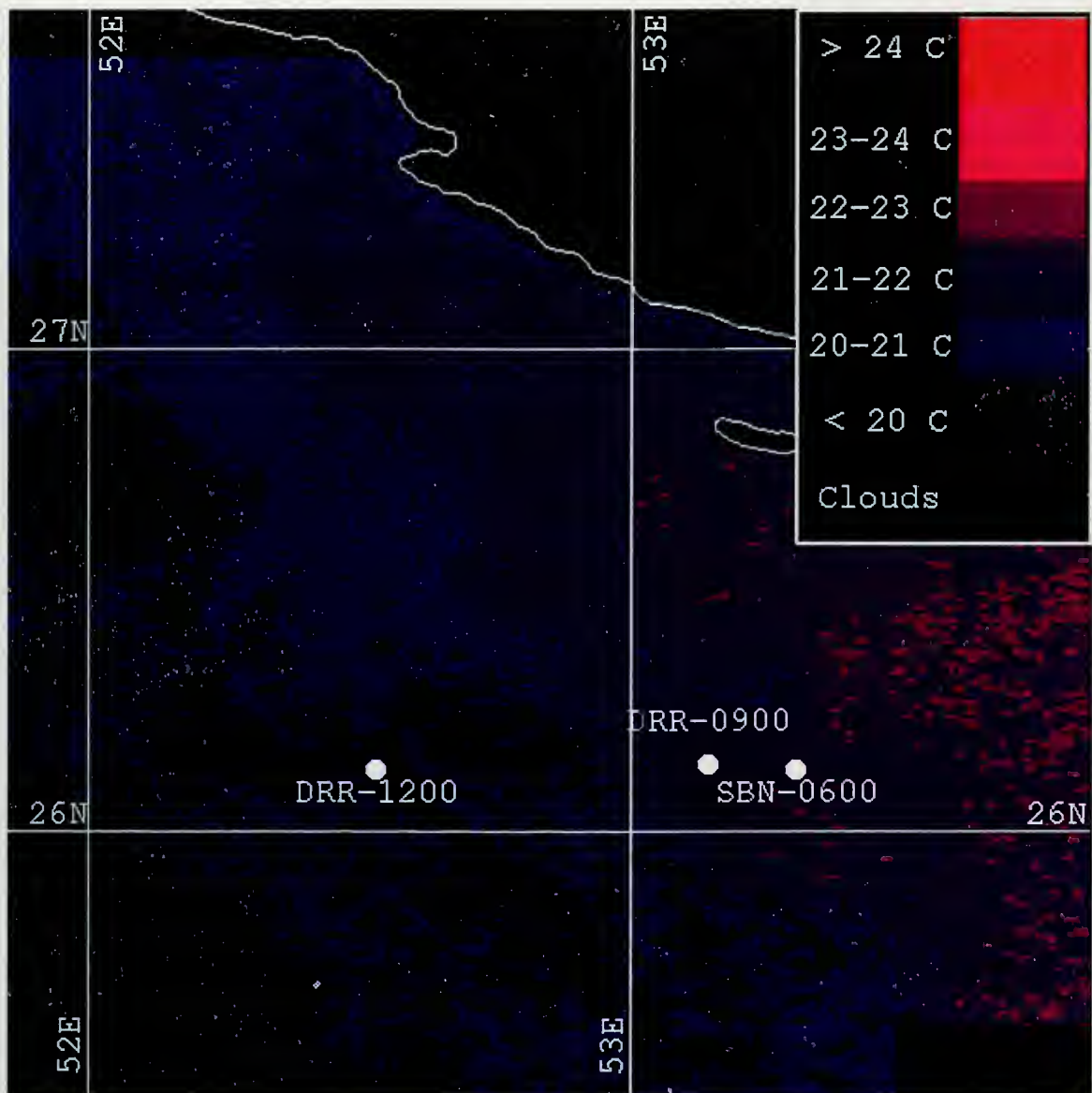
Figure 6: NOAA 14 AVHRR sea surface temperature image of the SHAREM 110 region at 1021z, 10 February 1995.
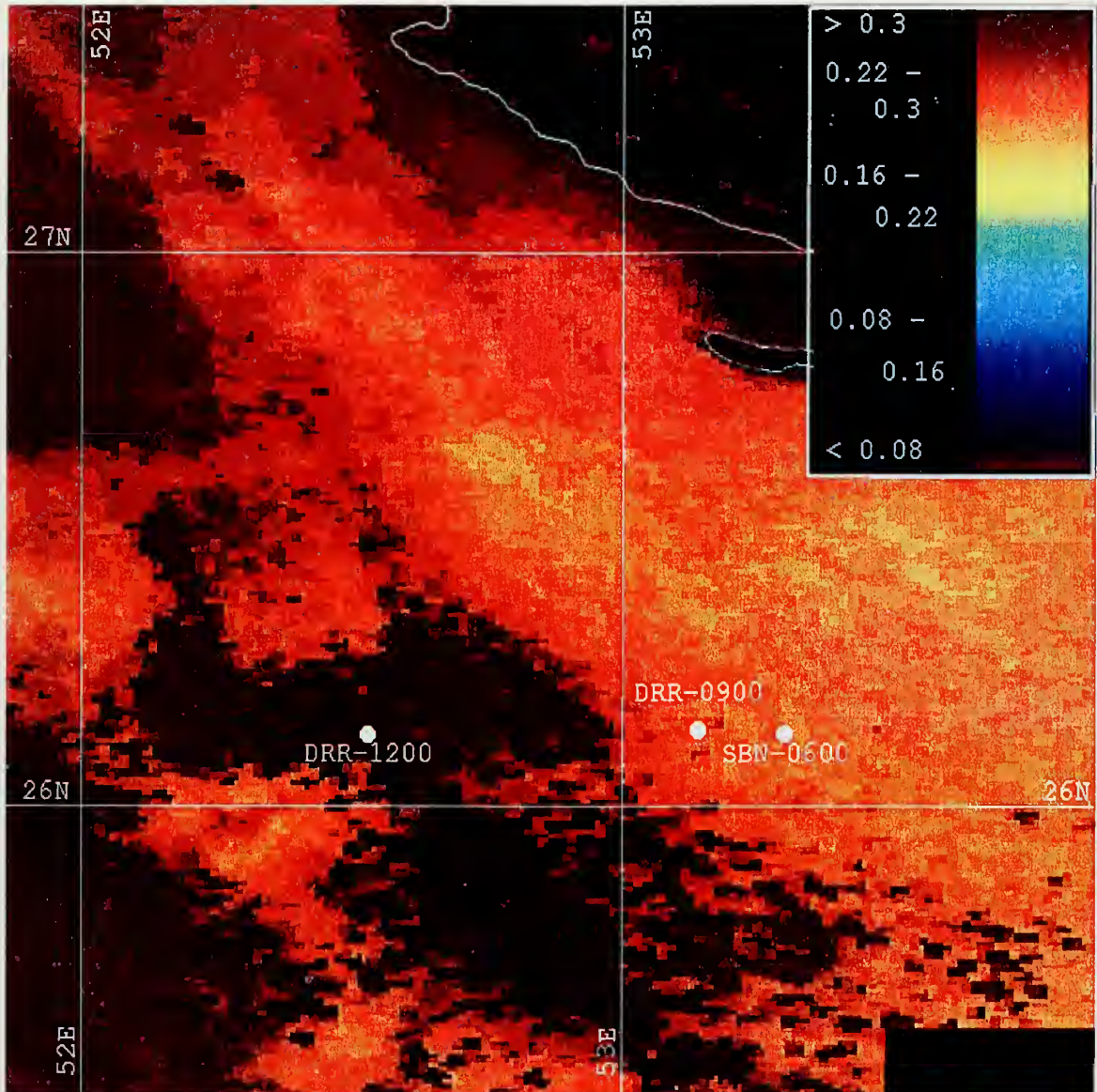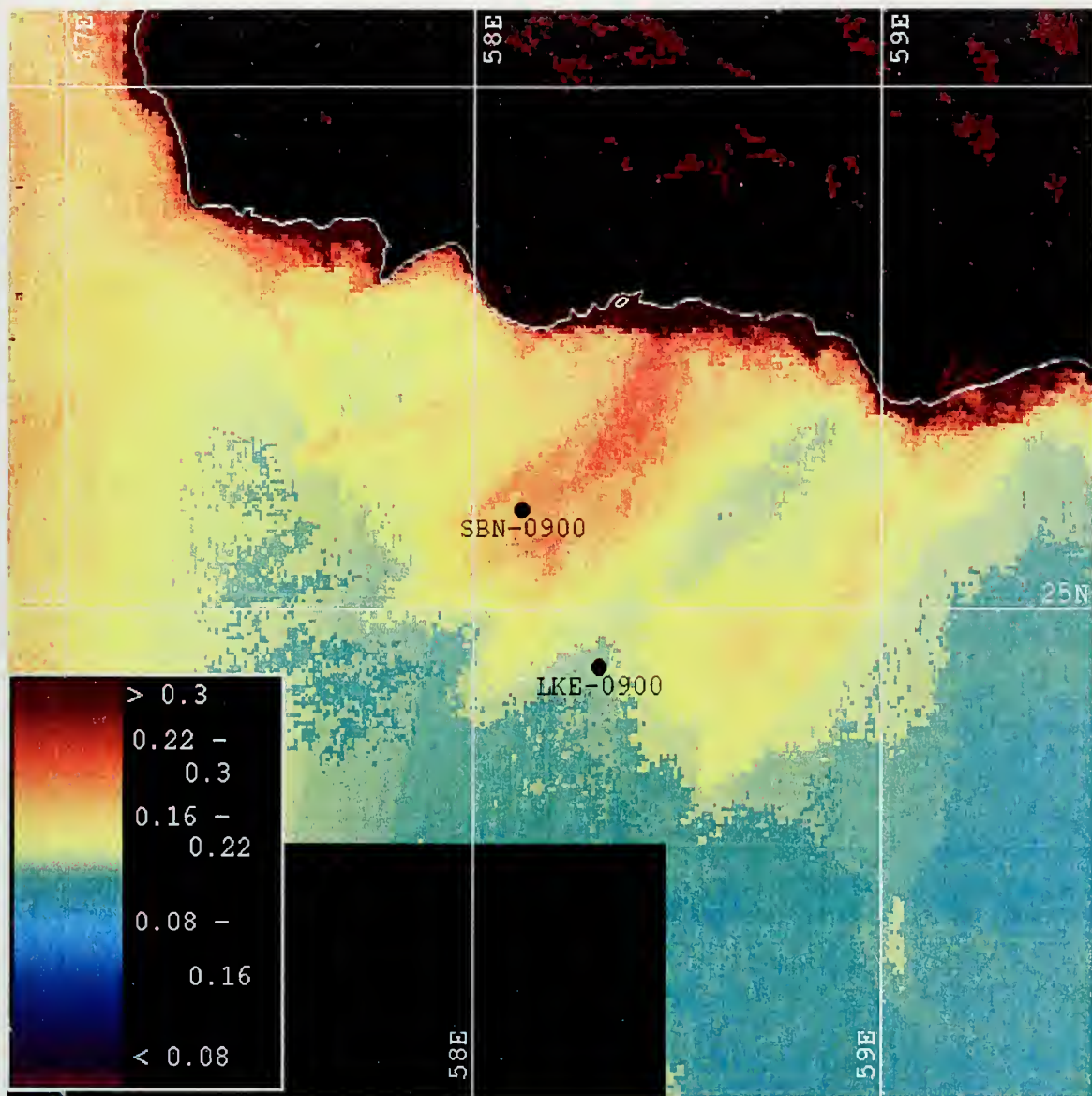
**Figure 7**: NOAA 14 AVHRR satellite-derived optical depth of the SHAREM 110 region at 1012z, 10 February 1995.
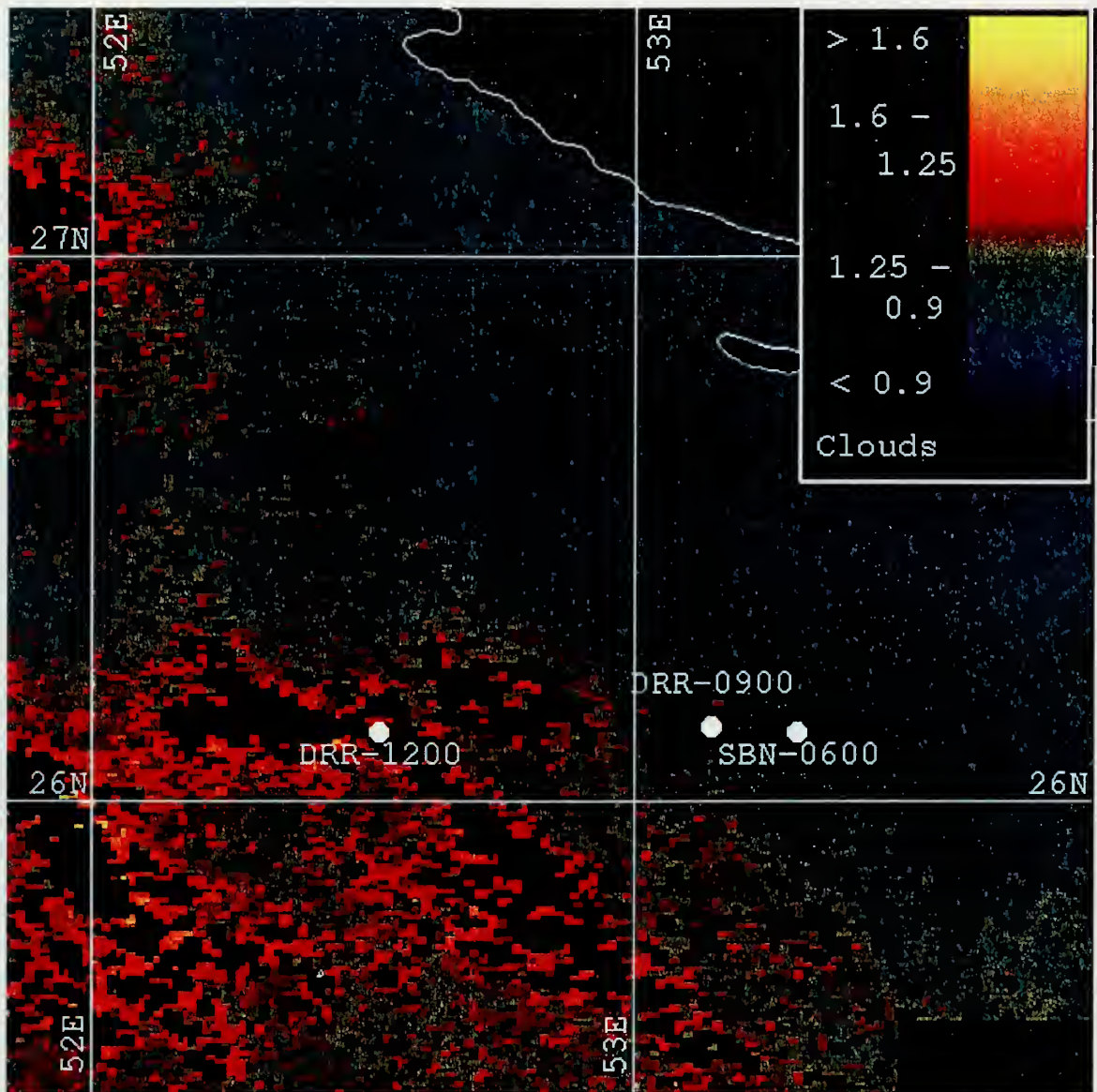
Figure 8: NOAA 14 AVHRR satellite-derived boundary layer height image of the SHAREM 110 region at 1021z, 10 February 1995. Heights in kilometers.
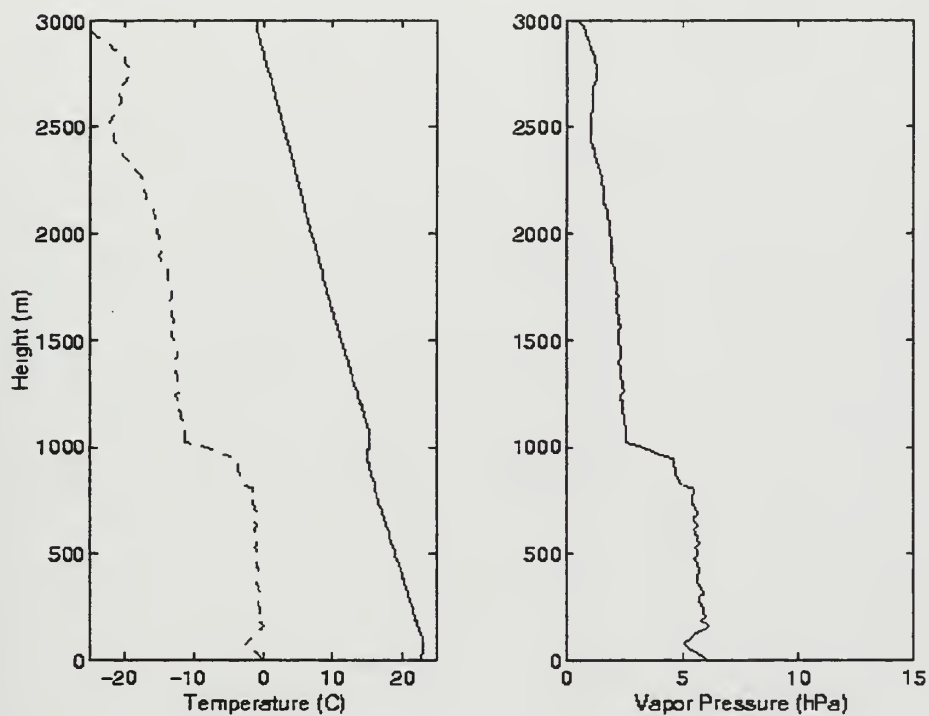
Figure 9: USNS Silas Bent, 0900z, 14 February 1995. Fig.
(a) shows vertical sounding and (b) shows vapor pressure
versus height (m). Note the low dew point temperatures and
low vapor pressure values. The atmosphere is very dry.
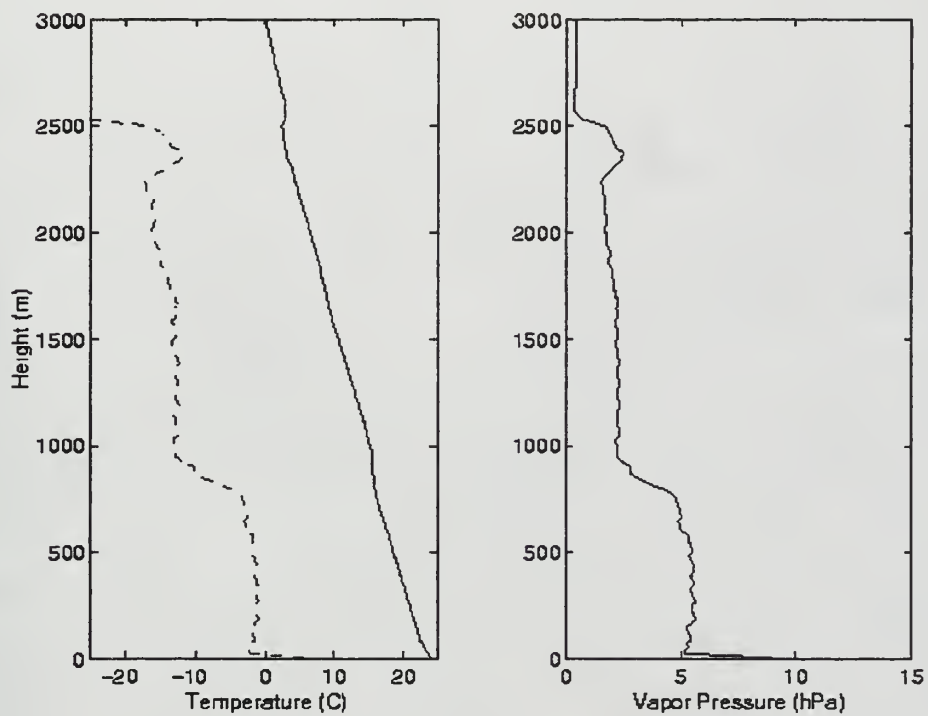
Figure 10: As in Figure 9 except for USS Lake Erie, 0900z, 14 February 1995.
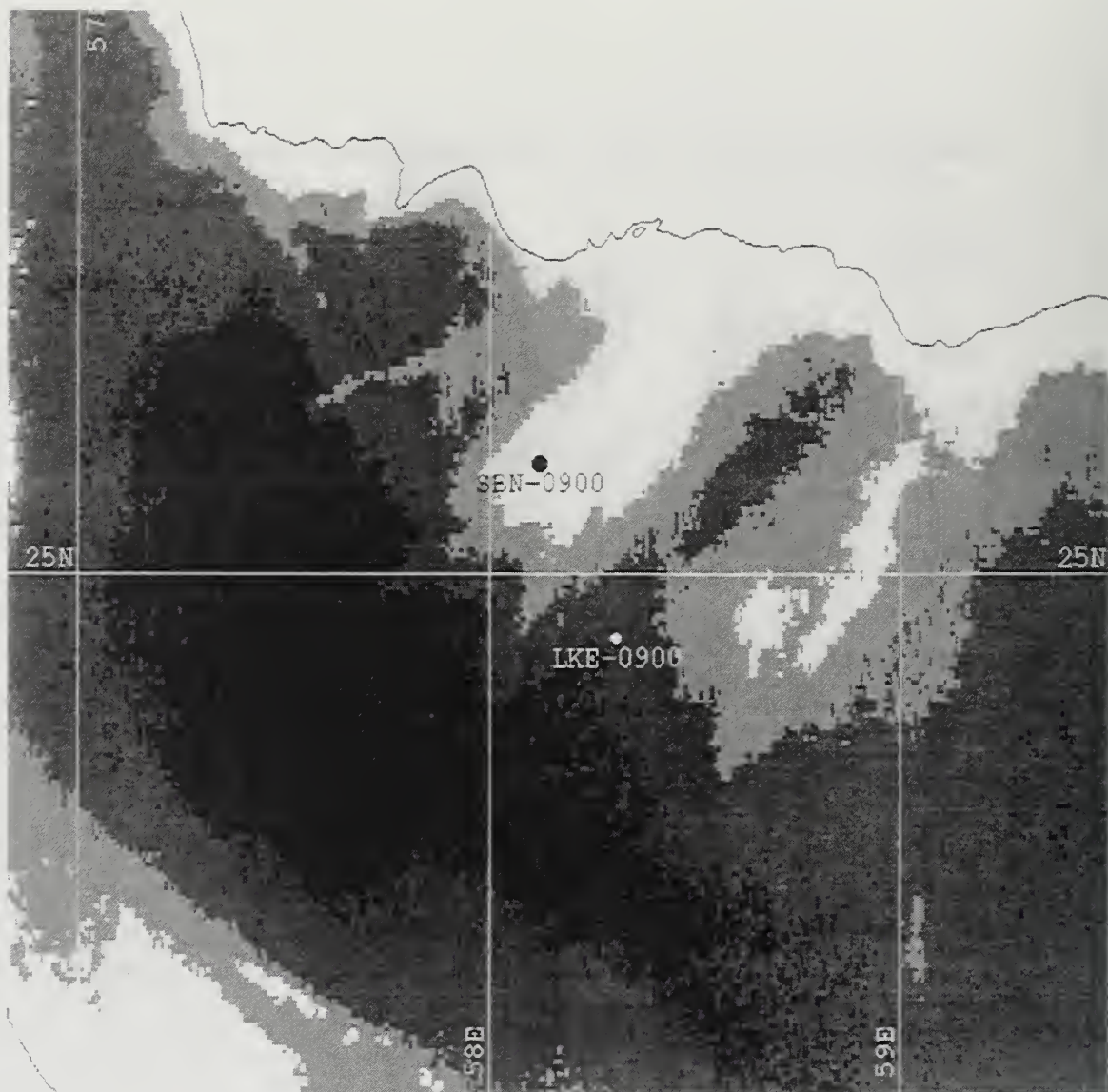
Figure 11: NOAA 14 AVHRR Channel 1 (visible) enhanced image of the SHAREM 110 Region at 0937z, 14 February 1995. Locations of USNS Silas Bent (SBN) and USS Lake Erie (LKE) and the time of soundings are indicated.
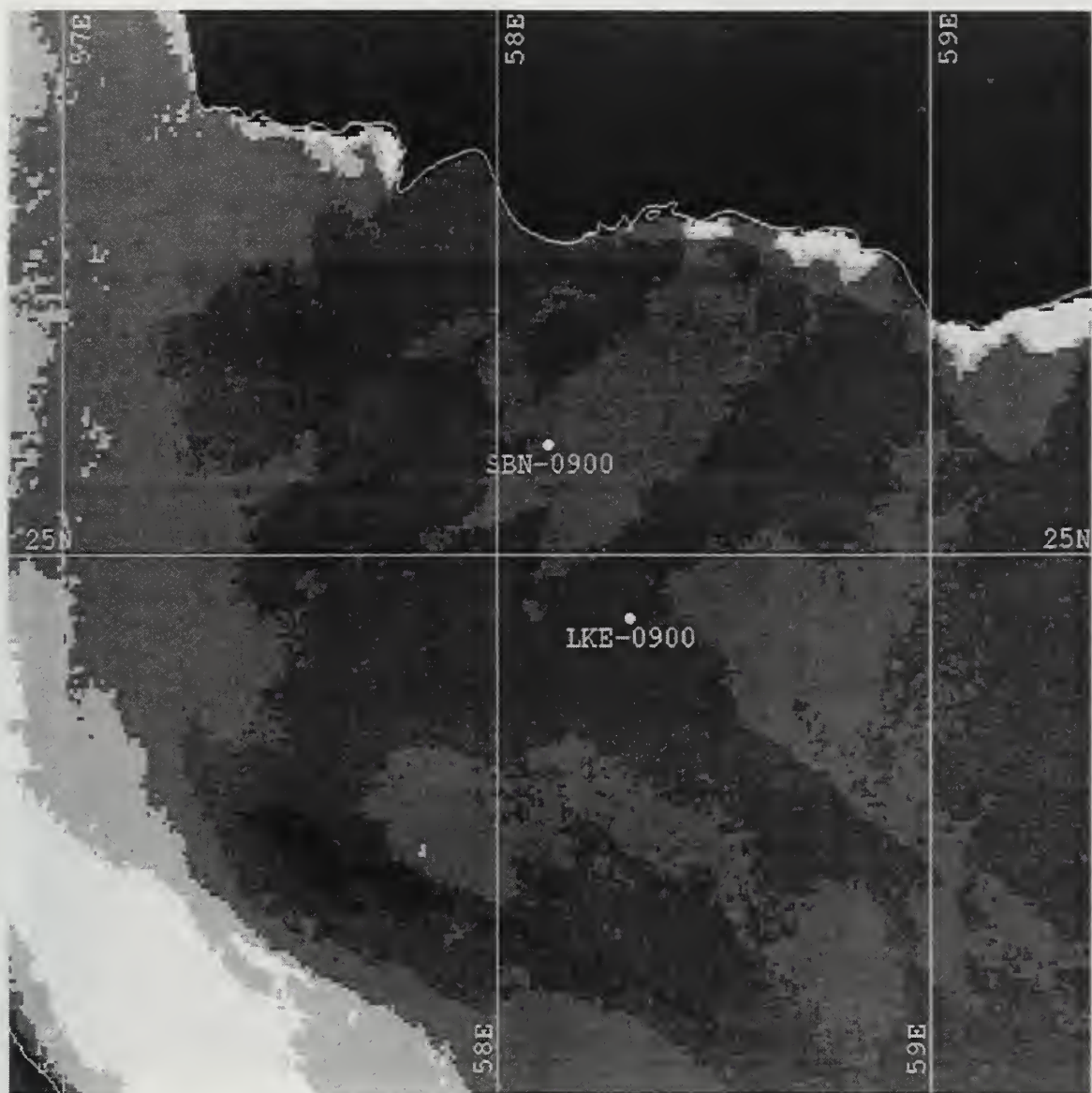
Figure 12: NOAA AVHRR Channel 4 (infrared) enhanced image of the SHAREM 110 region at 0937z, 14 February 1995.
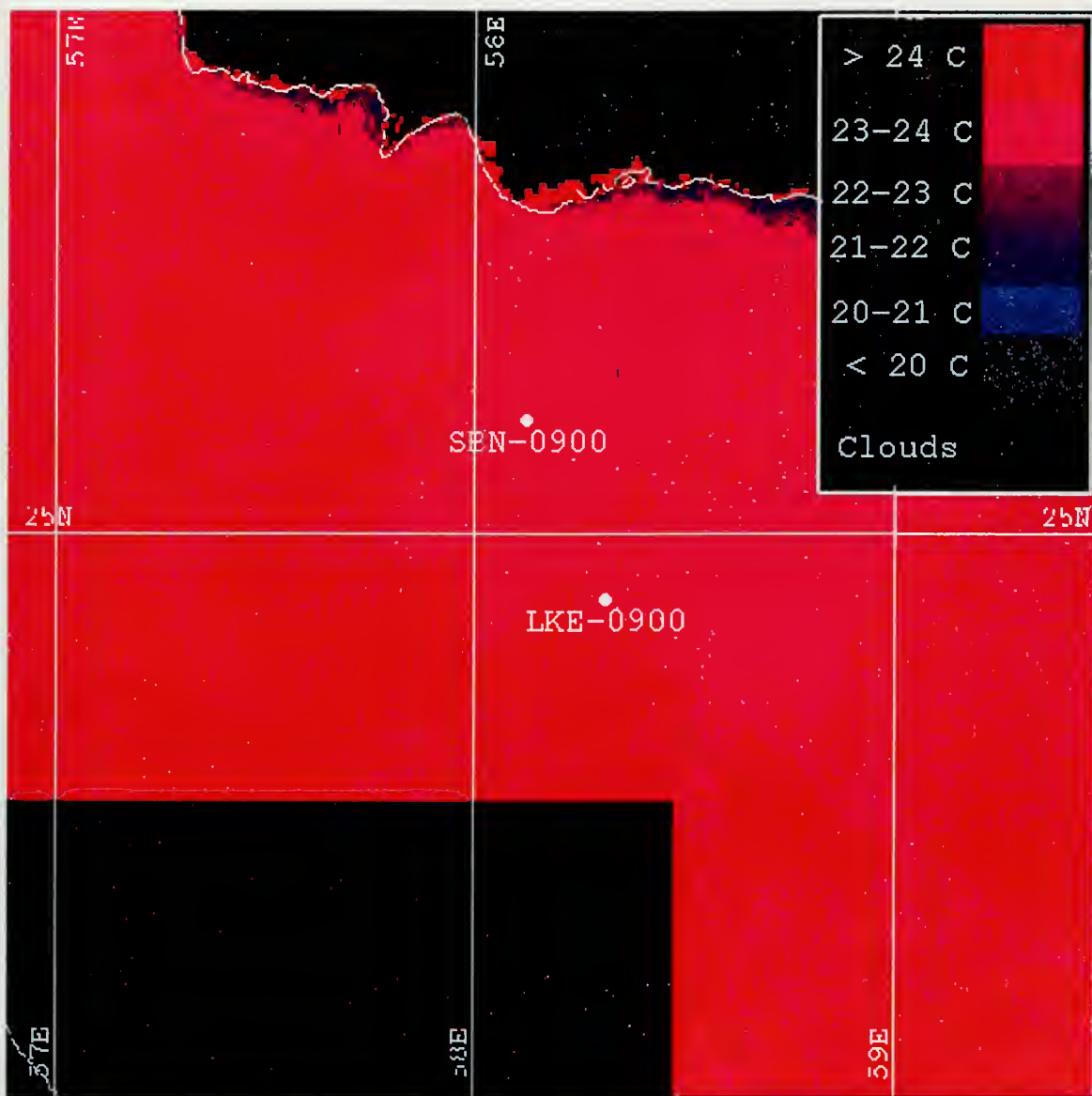
Figure 13: NOAA 14 AVHRR sea surface temperature image of the SHAREM 110 region at 0937z, 14 February 1995.

Figure 14: NOAA 14 AVHRR satellite-derived optical depth image of the SHAREM 110 region at 0937z, 14 February 1995.
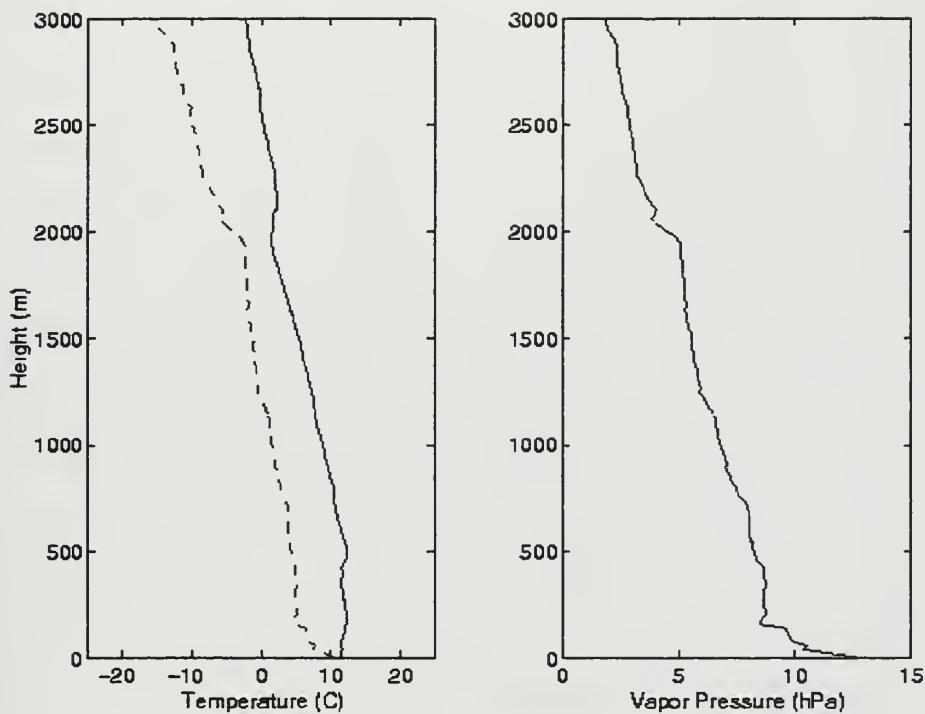
Figure 15: RV Pt Sur, 1500z, 16 May 1995. Fig (a) shows vertical sounding and (b) shows vapor pressure versus height (m). Note the two possible boundary layers. Lack of a clear cut layer can make interpretation difficult.
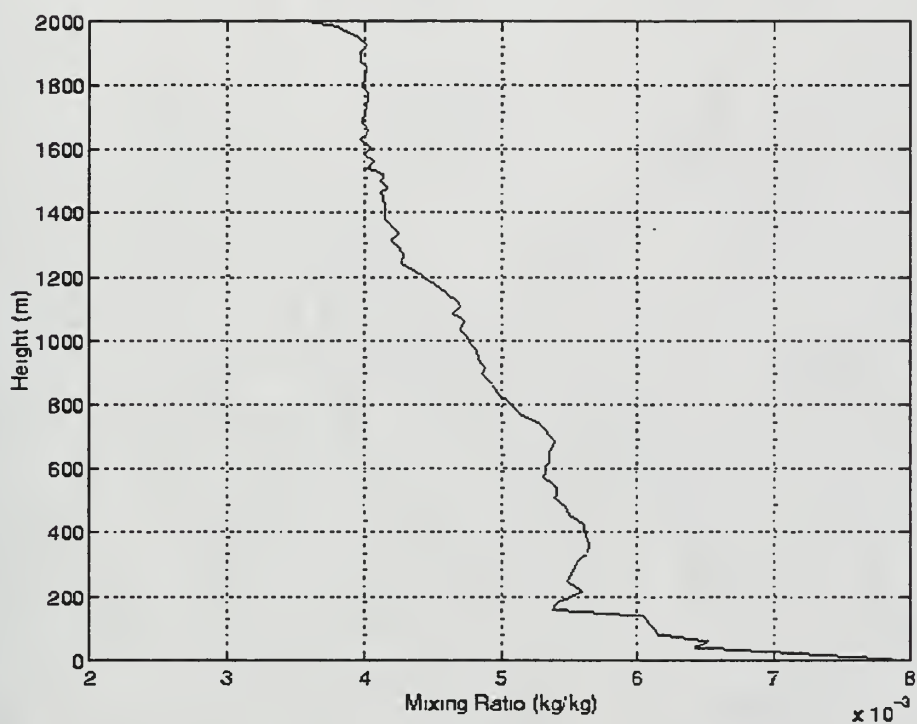
Figure 16: RV Pt Sur, 1500z, 16 May 1995. Mixing Ratio (kg/kg) versus height (m). Examining mixing ratio assists greatly in determining boundary layer position.
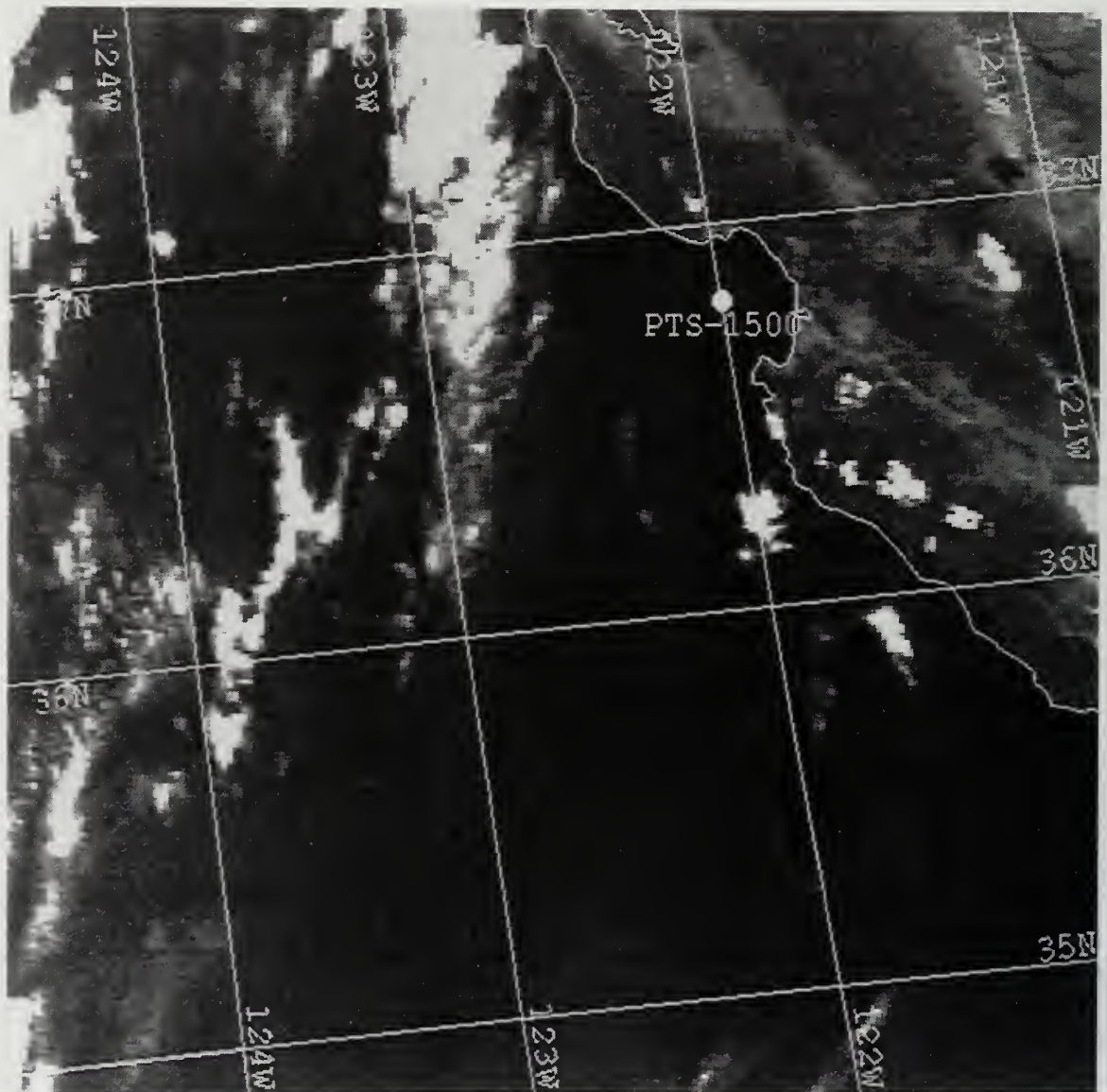
Figure 17: NOAA 12 AVHRR Channel 1 (visible) image of the
Monterey Bay region at 1512z, 16 May 1995. Location of
RV Pt Sur (PTS) and the time of sounding is indicated.
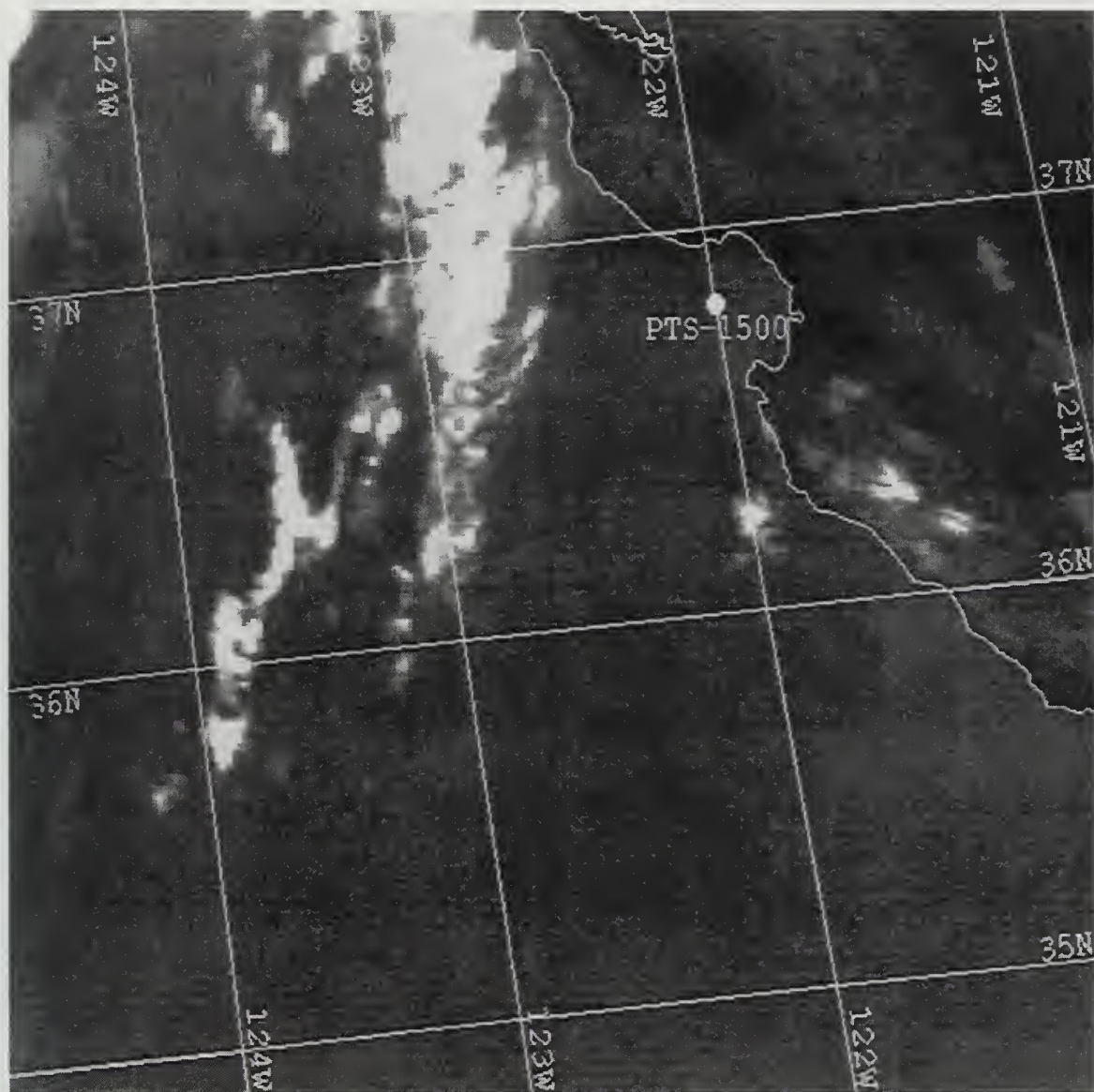
Figure 18: NOAA 12 AVHRR Channel 4 (infrared) image of the
Monterey Bay region at 1512z, 16 May 1995.
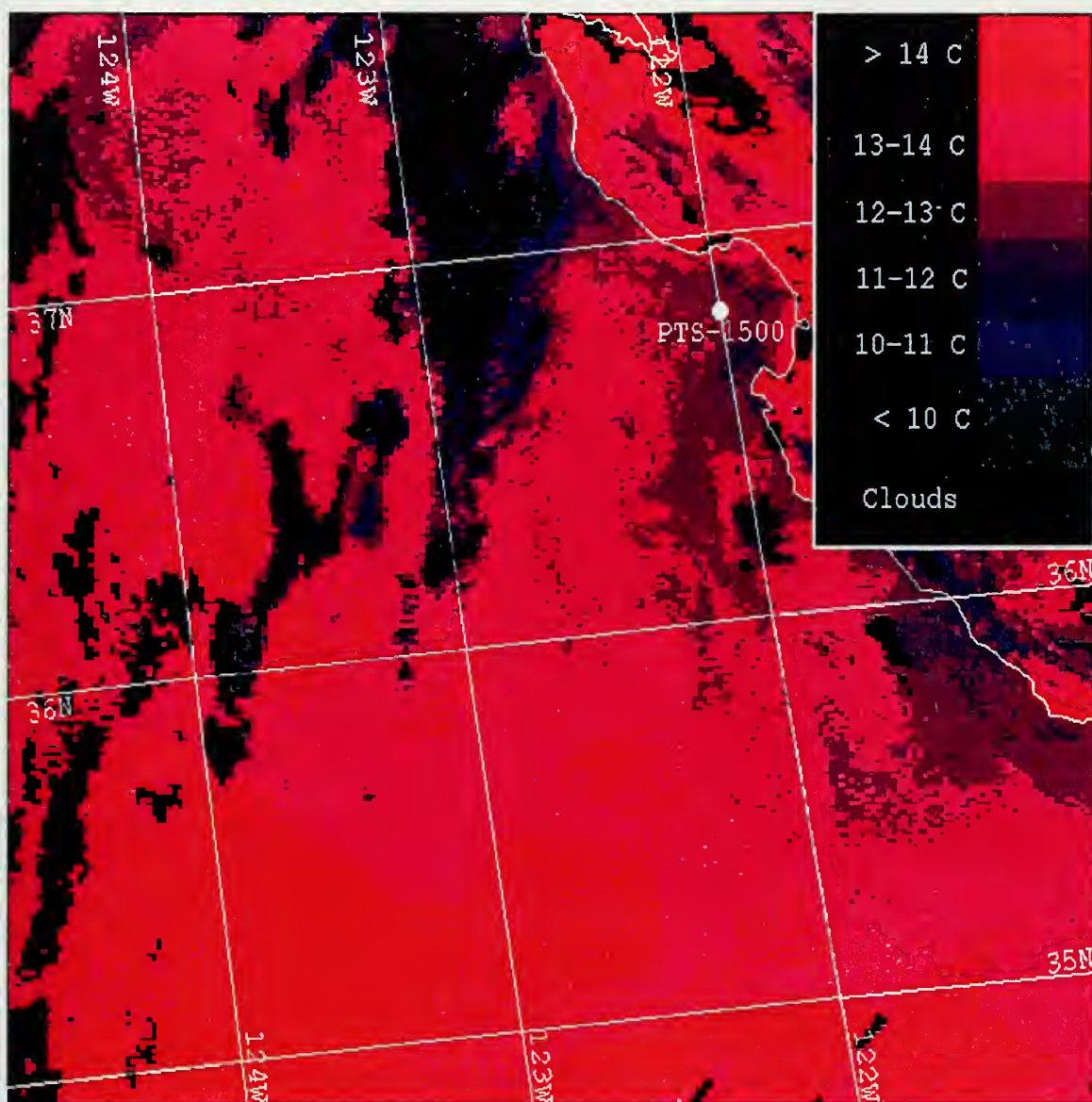
Figure 19: NOAA 12 AVHRR sea surface temperature image of the Monterey Bay region at 1512z, 16 May 1995.
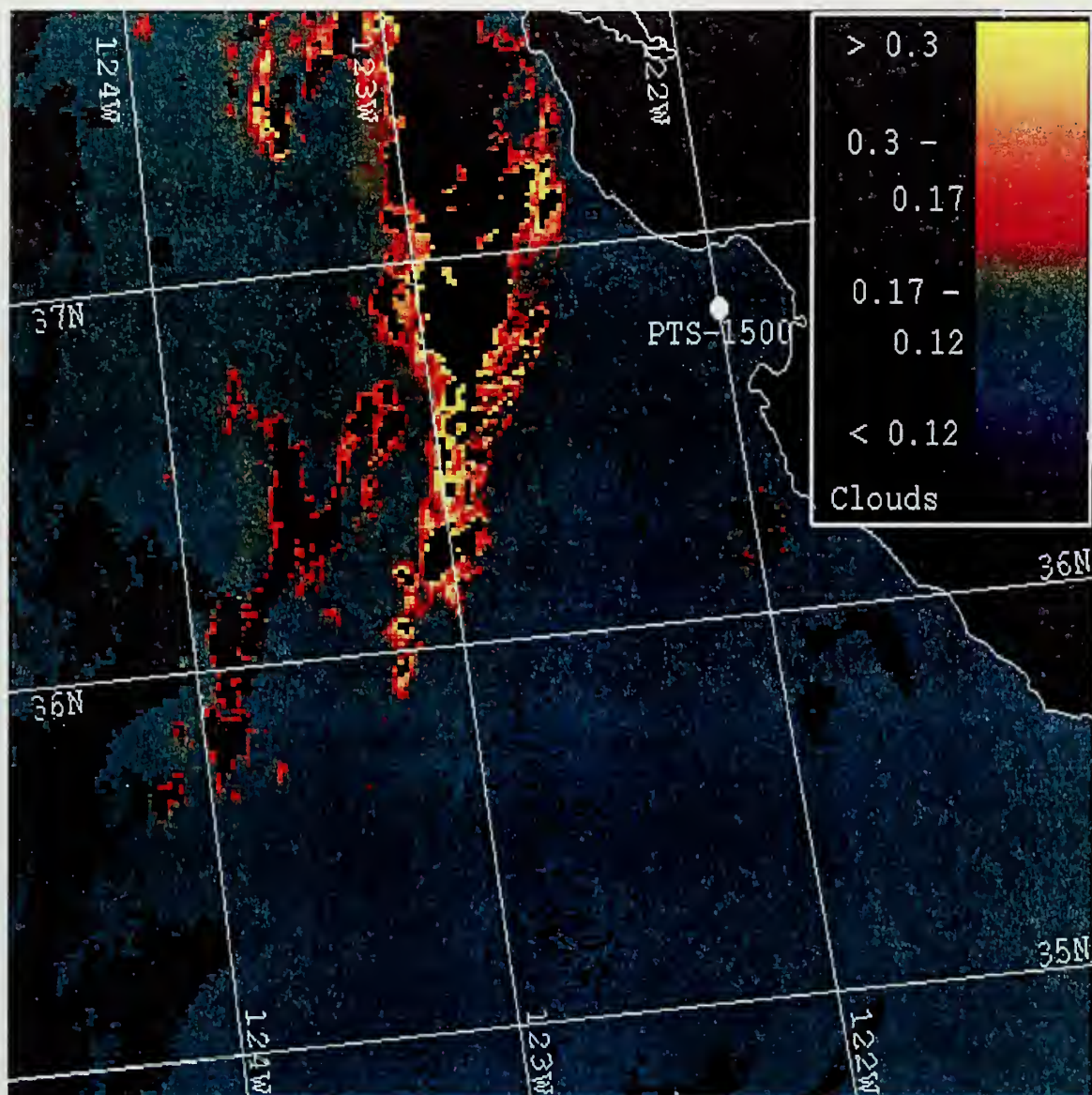
Figure 20: NOAA 12 AVHRR satellite-derived boundary layer
height image of the Monterey Bay region at 1512z,
16 May 1995. Heights in kilometers.
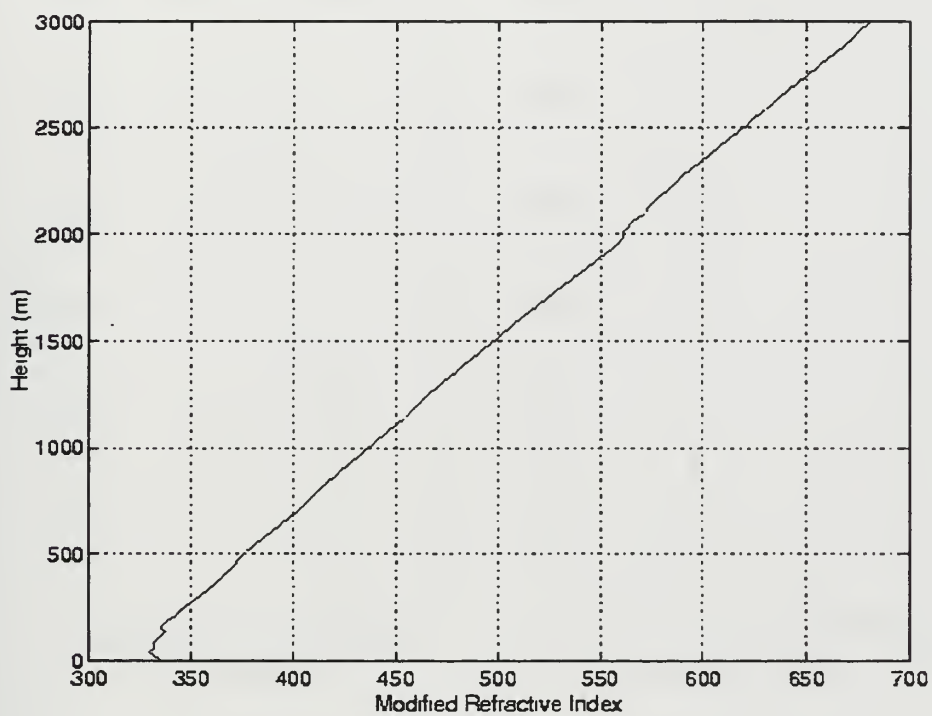
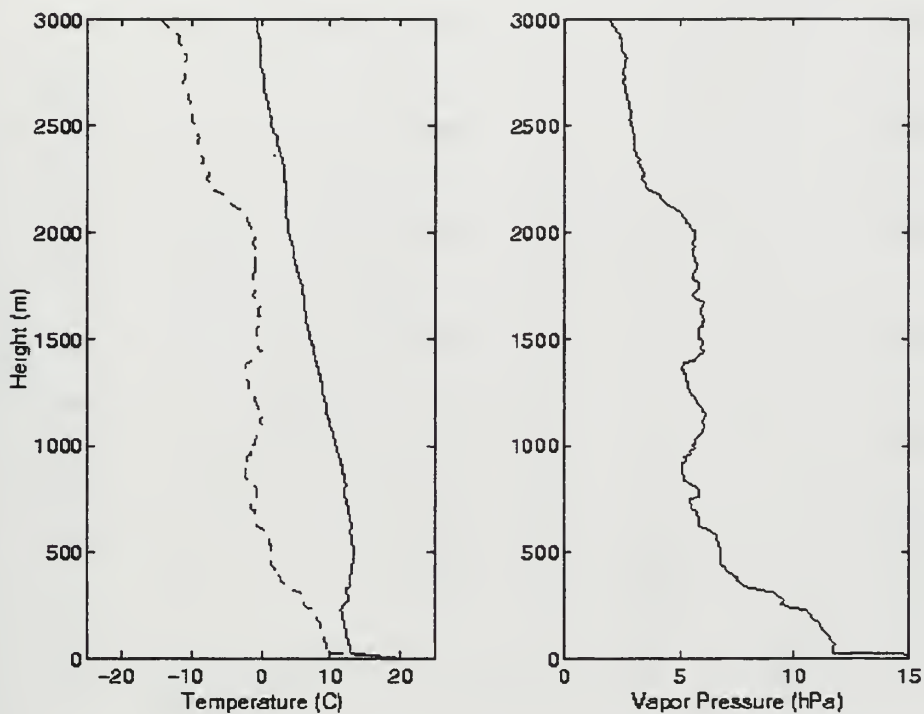**Figure 21**: M profile of RV Pt Sur, 1500z, 16 May 1995, sounding. Note the multiple layers.

Figure 22: RV Pt Sur, 2200z, 16 May 1995. Fig (a) shows vertical sounding and (b) shows vapor pressure versus height (m). Note the two possible boundary layers. Lack of a clear cut layer can make interpretation difficult.
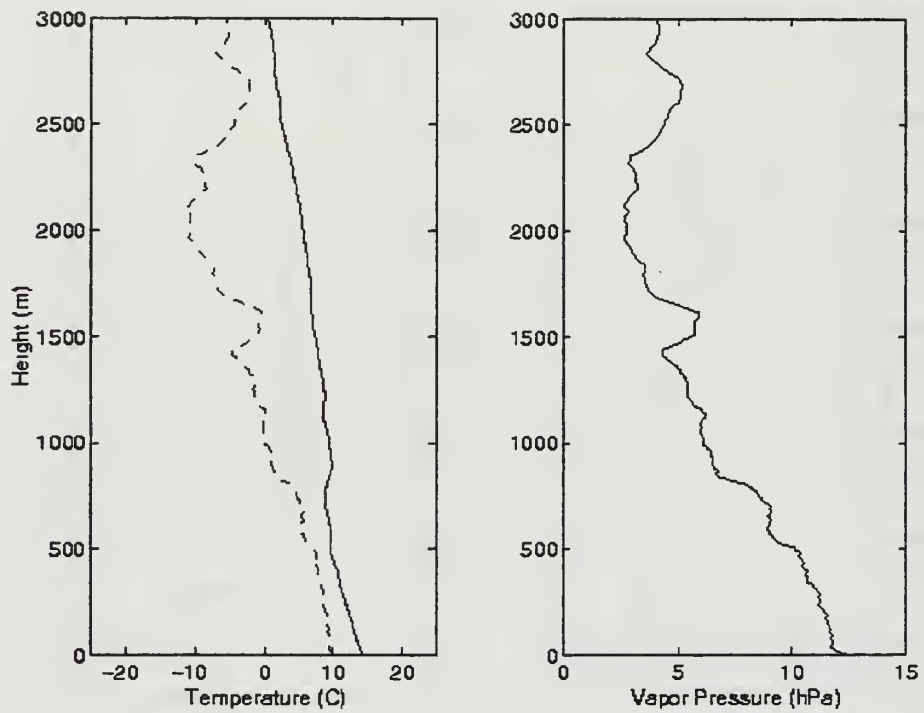
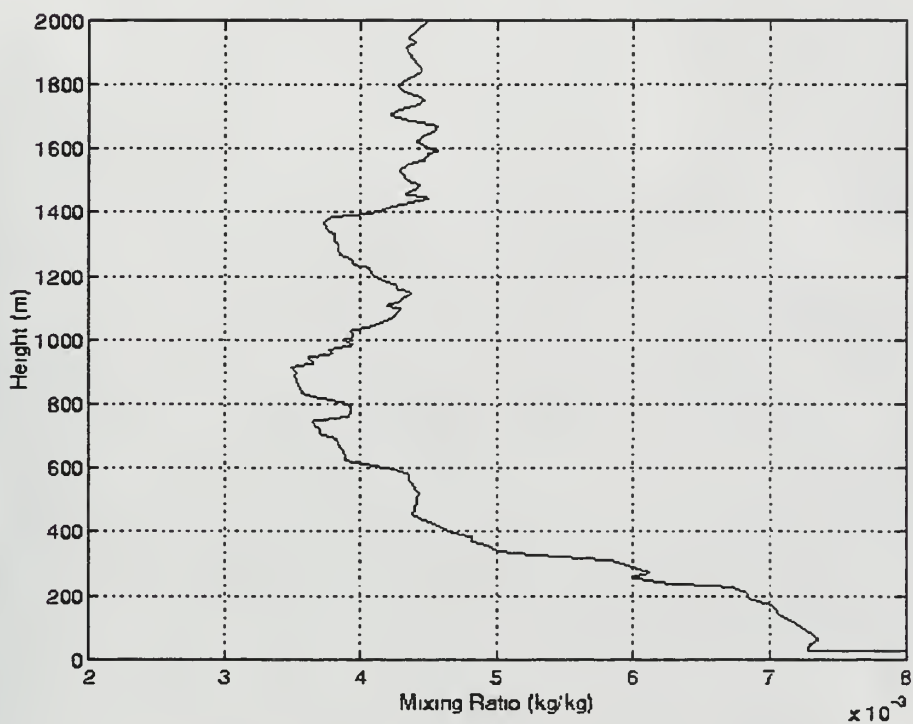**Figure 23**:   As in Fig 22 except for RV McArthur, 2200z, 16
May 1995.

Figure 24: RV Pt Sur, 2200z, 16 May 1995. Mixing Ratio (kg/kg) versus height (m). Fig (a) RV Pt Sur, Fig (b) RV McArthur. Examining mixing ratio assists greatly in determining boundary layer position.
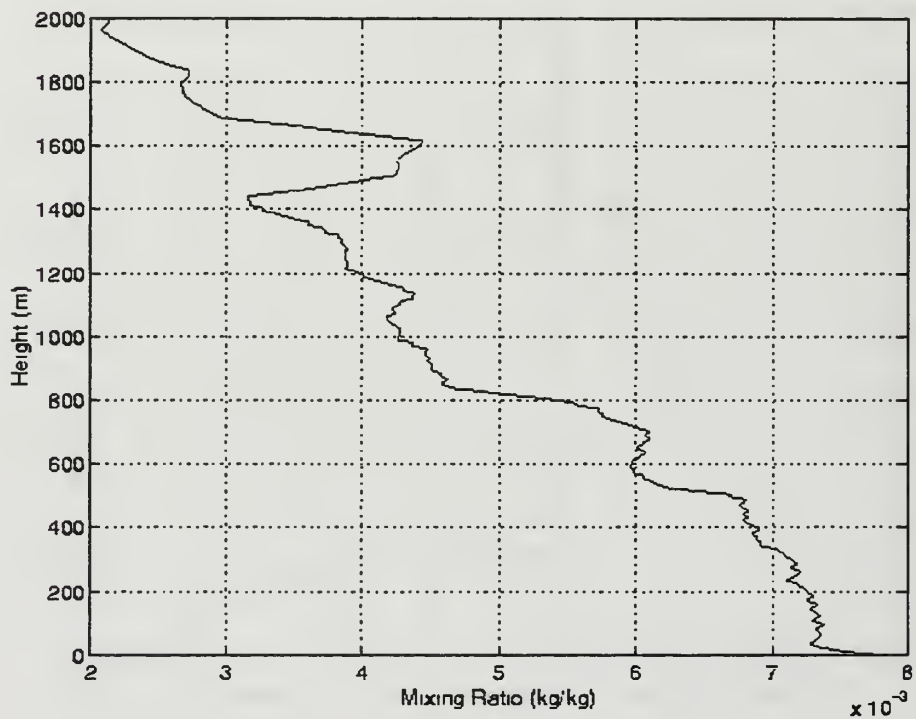
Figure 25: RV McArthur, 2200z, 16 May 1995. Mixing Ratio (kg/kg) versus height (m).
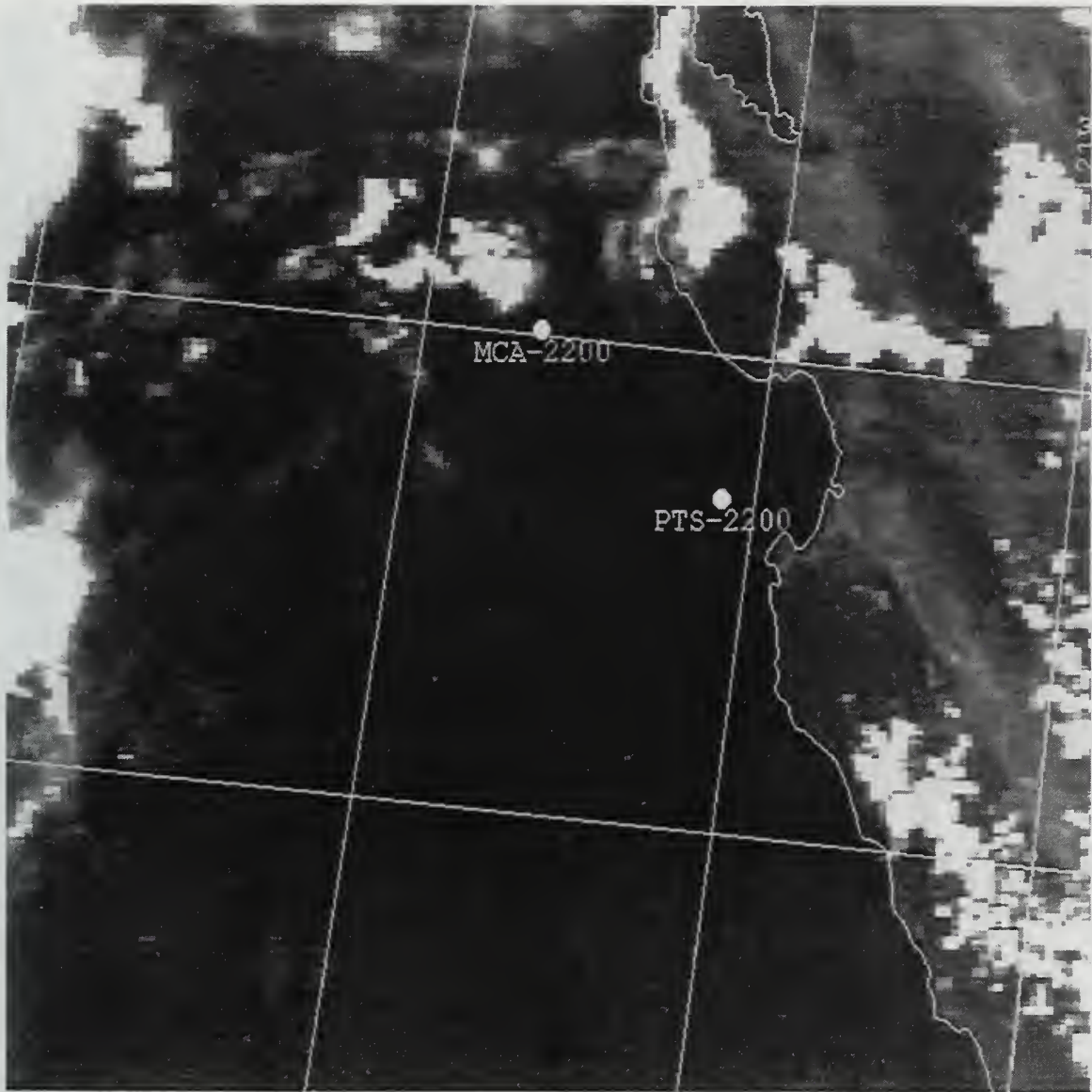
Figure 26: NOAA 14 AVHRR Channel 1 (visible) image of the
Monterey Bay region at 2204z, 16 May 1995. Location of
RV Pt Sur (PTS) and RV McArthur (MCA) and the time of
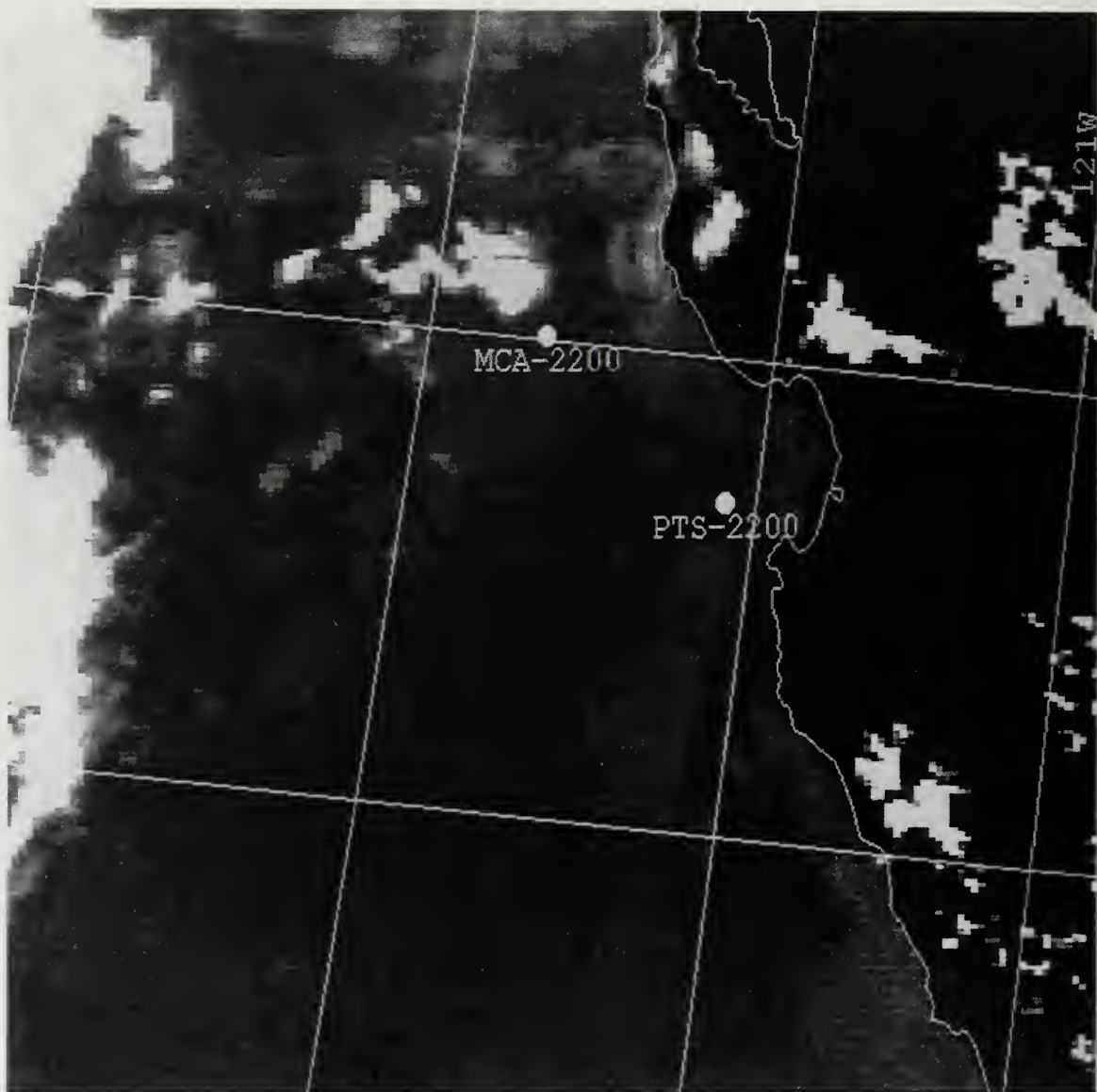soundings are indicated.

Figure 27: NOAA 14 AVHRR Channel 4 (infrared) image of the
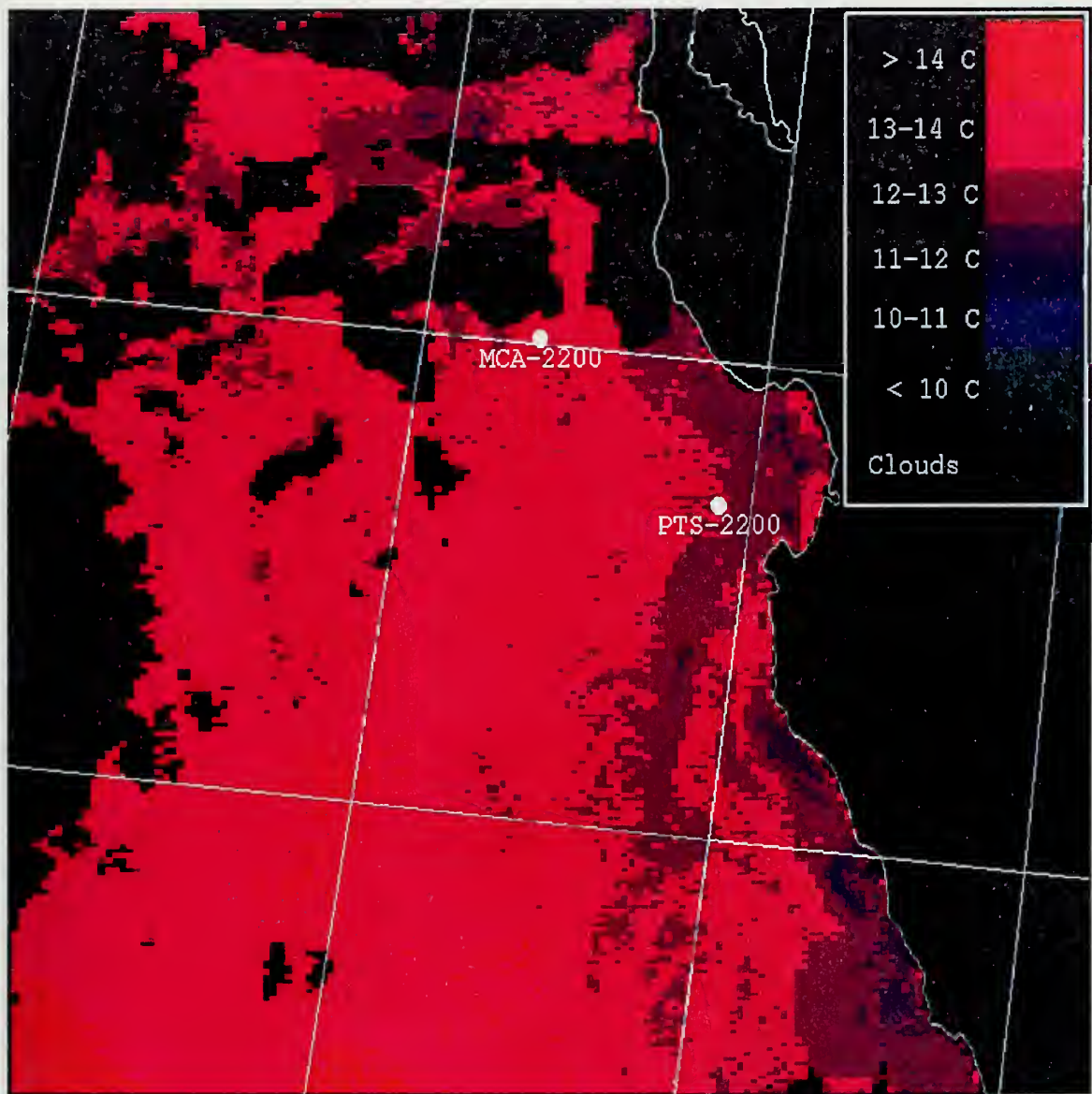Monterey Bay region at 2204z, 16 May 1995.

Figure 28: NOAA 14 AVHRR sea surface temperature image of the Monterey Bay region at 2204z, 16 May 1995.
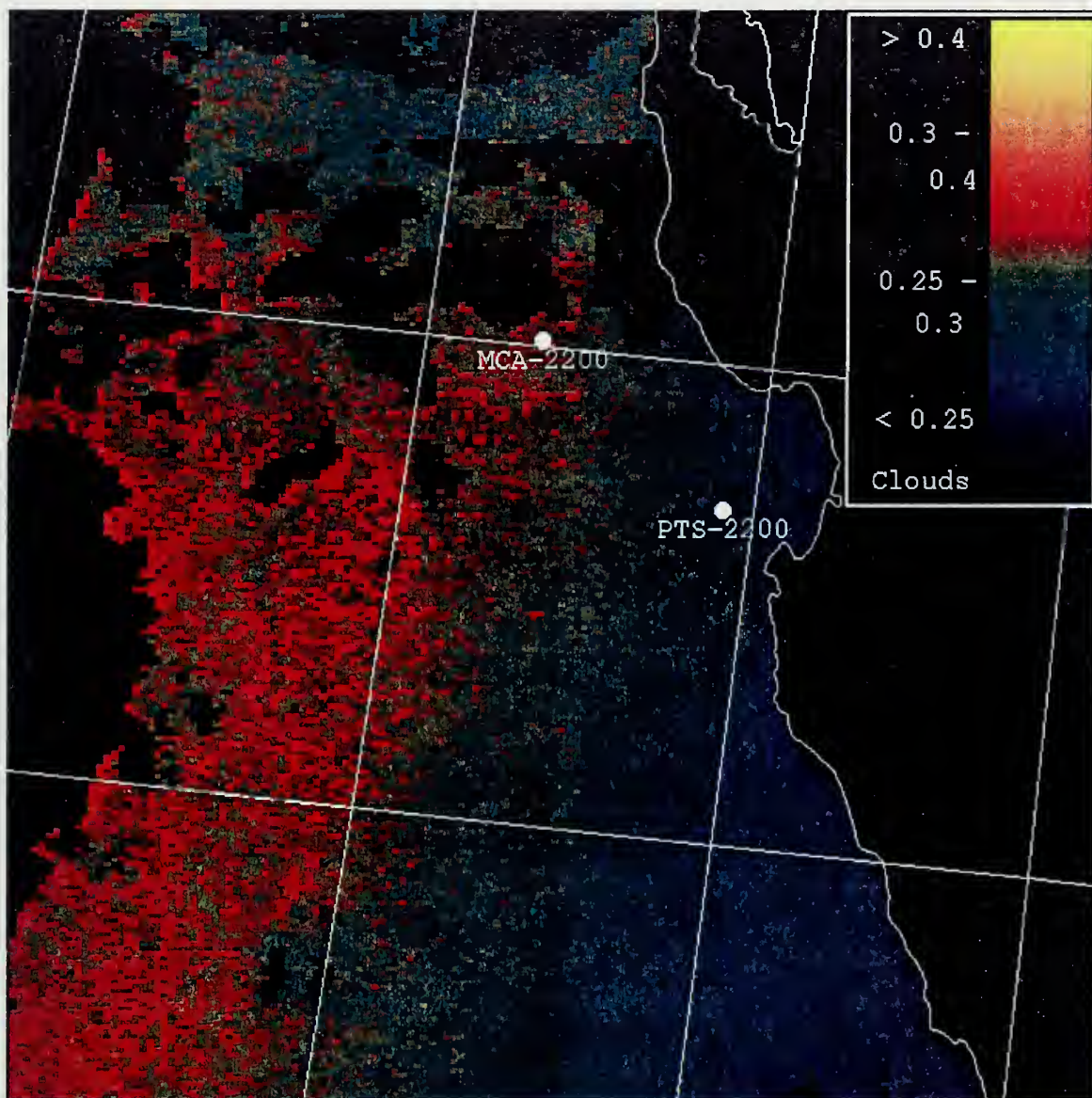
Figure 29: NOAA 14 AVHRR satellite-derived boundary layer
height image of the Monterey Bay region at 2204z,
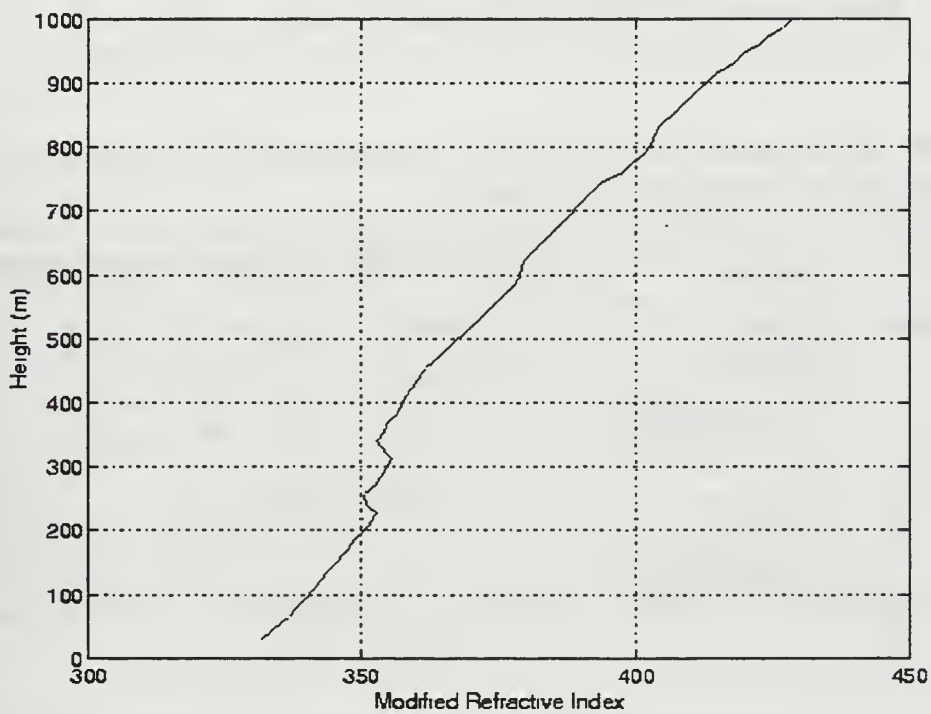16 May 1995. Heights in kilometers.

Figure 30: M profile of the RV Pt Sur 2200z, 16 May 1995, sounding.

Table I: SEA SURFACE TEMPERATURE COMPARISONS BETWEEN SATELLITE AND SHIP OBSERVATIONS. TEMPERATURES IN °C.

DATE	FROM	SILAS BENT	LAKE ERIE
10 FEB	N14	21.99	
	SHIP	21.11	
	DIFFERENCE	0.88	
14 FEB	N14	23.19	23.91
	SHIP	23.88	23.88
	DIFFERENCE	0.69	0.03

Table II: BOUNDARY LAYER HEIGHT COMPARISONS (SATELLITE VS RADIOSONDE). HEIGHTS IN METERS.

DATE	FROM	D.R. RAY	SILAS BENT	LAKE ERIE
10 FEB	N14	1005	1042	
	RAOB	1055	1090	
	DIFFERENCE	50	48	
14 FEB	N14		452	607
	RAOB		944	815
	DIFFERENCE		492	213

Table III: RESULTS OF APPLYING IR DUCT TECHNIQUE TO CLOUDY AREA OF THE IMAGE ON 10 FEBRUARY 1995. TEMPERATURES IN °C, HEIGHTS IN METERS.

LOCATION	T(cloud)	T(sea)	T(delta)	INV ALT
D.R. RAY (12z)	14.44	21.11	6.67	785
RAOB				818
DIFFERENCE				33

Table IV: SEA SURFACE TEMPERATURE COMPARISONS BETWEEN SATELLITE AND SHIP OBSERVATIONS. TEMPERATURES IN °C.

DATE	FROM	PT SUR	McARTHUR
16 MAY 1500z	N12	13.12	
	SHIP	12.7	
	DIFFERENCE	0.58	
16 MAY 2200z	N14	12.94	13.39
	SHIP	13.3	13.51
	DIFFERENCE	0.36	0.12

Table V: BOUNDARY LAYER HEIGHT COMPARISONS (SATELLITE VS RADIOSONDE). HEIGHTS IN METERS.

DATE	FROM	PT SUR	McARTHUR
16 MAY 1500z	N12	132	
	RAOB	139	
	DIFFERENCE	7	
16 MAY 2200z	N14	250	296
	RAOB	228	287
	DIFFERENCE	22	9

LIST OF REFERENCES

Durkee, P.A., 1984: *The Relationship Between Marine Aerosol Particles and Satellite-Detected Radiance.* Ph.D. Dissertation, Colorado State University, Fort Collins, CO.

Goroch, A.K., and Raby, J.W., 1995: *Analysis of Condensation Nuclei Counter Measurements in the Arabian Gulf and the Gulf of Oman*, Battlefield Environment Conference, Las Cruces, NM, 4 - 7 Dec. 1995.

Kren, R.J., 1987: *Estimation of Marine Boundary Layer Depth and Relative Humidity with Multispectral Satellite Measurements.* M.S. Thesis, Naval Postgraduate School, Monterey, CA.

Rosenthal, J., and Helvey, R., 1992: *Refractive Assessments from Satellite Observations*, AGARD CP-502, pp. 8.1 - 8.9.

Smolinski, S.P., 1988: *Marine Boundary Layer Depth and Relative Humidity Estimates Using Multispectral Satellite Measurements.* M.S. Thesis, Naval Postgraduate School, Monterey, CA.

Walsh, D.J., 1994: *Multispectral NOAA Marine Atmospheric Boundary Layer (MABL) Estimates During VOCAR.* M.S. Thesis, Naval Postgraduate School, Monterey, CA.

INITIAL DISTRIBUTION LIST

1. Defense Technical Information Center   2
    8725 John J. Kingman Rd., STE 0944
    Ft. Belvoir, VA 22060-6218

2. Library, Code 52   2
    Naval Postgraduate School
    Monterey, CA 93943-5101

3. Commander   1
    Space and Naval Warfare Systems Command (PMW-185)
    Washington D. C. 20363-5100
    Attn: CAPT W. Shutt

4. Naval Research Laboratory   1
    Naval Postgraduate School Annex
    Monterey, CA 93940-5006
    Attn: A. Goroch, Code 7542

5. Naval Research Laboratory   2
    Naval Postgraduate School Annex
    Monterey, CA 93940-5006
    Attn: J. Cook, Code 7542

6. Dr. Scott Sandgathe (ONR 322AM)   1
    Office of Naval Research
    Ocean, Atmosphere and Space Dept.
    800 N. Quincy St.
    Arlington, VA 22217-5600

7. Chairman (Code MR/HY)   1
    Department of Meteorology
    Naval Postgraduate School
    Monterey, CA 93943-5002

8. Professor Carlyle H. Wash (Code MR/WX)   2
    Department of Meteorology
    Naval Postgraduate School
    Monterey, CA 93943-5002

9.   Professor Kenneth L. Davidson   (Code MR/DS)   2
      Department of Meteorology
      Naval Postgraduate School
      Monterey, CA 93943-5002

10.   Professor Phillip Durkee   (Code MR/DE)   1
      Department of Meteorology
      Naval Postgraduate School
      Monterey, CA 93943-5002

11.   Analysis & Technology, Inc.   1
      2341 Jefferson Davis Highway
      Suite 1250
      Arlington, VA 22202
      Attn: M. Pastore

12.   Dr. Jeurgen Richter   (Code 54)   2
      NCCOSC RDT&E Division   (NRaD)
      53570 Silvergate Ave
      San Diego, CA 92152-5230

13.   Lieutenant Troy L. Teadt   1
      1276 Spruance Rd.
      Monterey, CA 93940